Food & Function

ROYAL SOCIETY OF CHEMISTRY

PAPER

View Article Online
View Journal | View Issue

Cite this: *Food Funct.*, 2023, **14**, 6496

Trans-palmitoleic acid, a dairy fat biomarker, stimulates insulin secretion and activates G protein-coupled receptors with a different mechanism from the *cis* isomer†

Eliza Korkus,[a] Marcin Szustak,[a] Rafal Madaj,[b,c] Arkadiusz Chworos,[b] Anna Drzazga,[a] Maria Koziołkiewicz,[a] Grzegorz Dąbrowski,[d] Sylwester Czaplicki,[d] Iwona Konopka[d] and Edyta Gendaszewska-Darmach *[a]

Dietary *trans*-palmitoleic acid (*trans* 16:1n-7, *t*POA), a biomarker for high-fat dairy product intake, has been associated with a lower risk of type 2 diabetes mellitus (T2DM) in some cross-sectional and prospective epidemiological studies. Here, we investigated the insulin secretion-promoting activity of *t*POA and compared them with the effects evoked by the *cis*-POA isomer (*c*POA), an endogenous lipokine biosynthesized in the liver and adipose tissue, and found in some natural food sources. The debate about the positive and negative relationships of those two POA isomers with metabolic risk factors and the underlying mechanisms is still going on. Therefore, we examined the potency of both POA isomers to potentiate insulin secretion in murine and human pancreatic β cell lines. We also investigated whether POA isomers activate G protein-coupled receptors proposed as potential targets for T2DM treatment. We show that *t*POA and *c*POA augment glucose-stimulated insulin secretion (GSIS) to a similar extent; however, their insulin secretagogue activity is associated with different signaling pathways. We also performed ligand docking and molecular dynamics simulations to predict the preferred orientation of POA isomers and the strength of association between those two fatty acids and GPR40, GPR55, GPR119, and GPR120 receptors. Overall, this study provides insight into the bioactivity of *t*POA and *c*POA toward selected GPCR functions, indicating them as targets responsible for the insulin secretagogue action of POA isomers. It reveals that both *t*POA and *c*POA may promote insulin secretion and subsequently regulate glucose homeostasis.

Received 7th November 2022,
Accepted 5th June 2023

DOI: 10.1039/d2fo03412c

rsc.li/food-function

1. Introduction

With type 2 diabetes mellitus (T2DM) on the rise, there is a growing need to develop dietary strategies regulating glucose homeostasis. Dairy ingredients that have been identified to be beneficial for T2DM include flavonoids, calcium, probiotics, vitamins K-1 and K-2, branched-chain amino acids, medium-chain and odd-chain saturated fats, and unsaturated fats.[1] Among them, milk fat fatty acids (FAs) are considered important nutritional components and have a significant impact on human health.[2] On the presence of fat in milk, the U.S. dietary guidelines recommend the consumption of fat-free or low-fat milk and milk products.[3] However, there is very little evidence that high-fat dairy consumption is more harmful than low-fat dairy intake in terms of T2DM risk. What is more, the meta-analysis of 13 cohort studies showed no link between high-fat dairy consumption and T2DM risk.[4]

Among dairy fatty acids, *trans*-palmitoleic acid (*t*POA), containing one double bond located at the n-7 position using the Ω-nomenclature (C16:1 n-7), may act as a biomarker of metabolic health manifested as improved glucose and insulin concentrations, insulin sensitivity measured using the homeostasis assessment model of insulin resistance (HOMA-IR) index, fasting insulinemia and fasting glycemia, glucose uptake by muscles and liver, blood lipids, and inflammatory markers.[5,6] *trans*-POA, also known as "palmitelaidic acid" in the literature, is mainly found in naturally occurring ruminant-derived dairy

[a]*Faculty of Biotechnology and Food Sciences, Institute of Molecular and Industrial Biotechnology, Lodz University of Technology, Stefanowskiego 2/22, 90-537 Lodz, Poland. E-mail: edyta.gendaszewska-darmach@p.lodz.pl*
[b]*Division of Bioorganic Chemistry Centre of Molecular and Macromolecular Studies, Polish Academy of Sciences, Sienkiewicza, 112, 90-363 Lodz, Poland*
[c]*Institute of Evolutionary Biology, Faculty of Biology, Biological and Chemical Research Centre, University of Warsaw, Żwirki i Wigury 101, 02-089 Warsaw, Poland*
[d]*Faculty of Food Sciences, Chair of Plant Food Chemistry and Processing, University of Warmia and Mazury in Olsztyn, Pl. Cieszyński 1, 10-957 Olsztyn, Poland*
† Electronic supplementary information (ESI) available. See DOI: https://doi.org/10.1039/d2fo03412c

and meat *trans* fats. Noteworthily, ruminant *trans* fatty acids (rTFAs) are generated by bacteria from linoleic and α-linolenic acids in the animal gut. The chain of *trans* vaccenic acid (18:1, n-7), the most abundant rTFA, can be shortened to *t*POA.[7] The concentration of *t*POA is typically between 1 and 2% when the cows are on indoor feeding and between 2 and 4% when they are on fresh pasture.[8] Alternatively, *t*POA could also be produced by the ruminant biohydrogenation of dietary C16:3 n-3 fatty acids found in "C16:3 plants".[5] The minor presence of *t*POA in dairy products was reported to be 0.05%, 0.04%, and 0.08% of total fatty acids in cow, ewe, and goat milk, respectively.[9] Very recently, ruminant fats were shown to be the only contributors to circulating levels of *t*POA in humans where partially hydrogenated oils are not used anymore, *e.g.*, in France.[10] What is more, the circulating plasma levels of *t*POA ranging from 0.02% to 0.55% of total fatty acids[11] can be explained mainly by its dietary origin and are positively correlated with self-reported consumption of whole-fat dairy, butter, margarine, and baked desserts.[5] Furthermore, recent studies directly showed that supplementation with sea buckthorn oil augmented with *t*POA increased the serum phospholipid *t*POA by 26.6% at a dose of 480 mg per day.[12]

The majority of data on the physiological effects of dietary *t*POA comes from epidemiological studies, which are, however, inconsistent regarding the influence on T2DM risk. Nonetheless, Mozaffarian *et al.* patented the use of dietary *t*POA to treat insulin resistance.[13] Indeed, some cross-sectional and prospective epidemiological studies have suggested that dietary *t*POA has beneficial effects on the risk of T2DM and could prevent insulin resistance by reducing insulinemia.[14,15] However, in other studies, *t*POA was not associated with T2DM outcomes in fully adjusted models comprising age, sex, and ethnicity (model 1), physical activity and total energy intake (model 2), total dairy or total hydrogenated food intake (model 3), and body mass index (model 4).[16] Furthermore, higher *t*POA proportions in the erythrocyte membrane predicted a significantly increased risk of diabetes.[17] These controversial results underline the need to unravel potential mechanisms of action of dietary *t*POA. Concerning T2DM, very recently Chávaro-Ortiz *et al.* reported the effect of *t*POA on glucose homeostasis in a C57BL/6 mouse model of diet-induced obesity during supplementation with *t*POA (3 g kg^{-1} diet) for 11 weeks. Although *t*POA prevented weight gain, it had a neutral influence on glucose homeostasis measured by glucose and insulin tolerance tests and insulin-mediated Akt activation.[18] Noteworthily, these findings contradict the results from clinical studies[15] that found increased insulin sensitivity in association with a higher serum *t*POA content which further supports the need for comparative studies between human and rodent models. However, also, little data exist on *in vitro* studies. Studies with the perfused pancreas isolated from male Sprague-Dawley rats revealed a three-fold stimulation of insulin release from the fasted pancreas in response to palmitoleic acid.[19] The second report refers to research with the INS-1 β cell line. *t*POA did not affect pancreatic duodenal homeobox factor 1 (*pdx1*) expression under chronic high glucose (20 mM) treatment but under basal (5.5 mM) glucose conditions, *t*POA demonstrated a stimulatory effect. Also, *t*POA increased the peroxisome proliferator-activated receptor γ activity.[20]

Importantly, palmitoleate can be found in nature as *cis* (*c*POA) and *trans* geometrical isomers. Endogenous *c*POA is synthesized in the human body primarily in the liver and secondarily in adipose tissue by desaturation of palmitic acid.[11,21] Subcutaneous adipose tissue triacylglycerols (TAGs) contain approximately 7.2 mol% of *c*POA, which means that *cis* 16:1n-7 is the second most abundant monounsaturated fatty acid after oleic acid.[22] Dietary *c*POA is present in modest amounts in some plant and animal-based foods; however, its overall nutritional intake is low (<4% of total energy).[23] However, *c*POA is highly concentrated in the sea buckthorn (*Hippophae sp.*) pulp oil, where it accounts for up to 52% of total fatty acids.[24] The *cis* isoform of POA has been associated with increased insulin sensitivity and suppression of hepatosteatosis.[21] Very recently, we have shown that the stimulatory effect of sea buckthorn pulp oil concerning insulin secretion from human islet EndoC-βH1 cells has been associated with the activity of FFAs acting as ligands of pancreatic G protein-coupled receptors (GPCRs). In particular, the presence of *c*POA seems to have the highest triggering effect.[25]

Concomitantly, the link between the fatty acid structure (double bond configuration) and function is critical[26,27] but similar or adverse functions of *c*POA and *t*POA have never been compared directly in terms of insulin secretion and GPCR activation. Therefore, the aim of this study was to answer the question if POA *trans* and *cis* isomers similarly stimulate insulin secretion. Consequently, we employed two pancreatic β cell lines of different derivations: MIN6 (a mouse insulinoma cell line) and EndoC-βH1 (a human cell line that closely mimics the functional properties of normal human β cells).[28] We also determined whether POA isomers activate GPCRs in a similar way, which were previously shown to mediate insulin secretion. As potential receptor targets, we chose GPR40, GPR55, GPR119, and GPR120 activated by free fatty acids and lipids containing fatty acid residues.[29] Such information will be helpful in understanding the biological roles of *c*POA and *t*POA and to come closer to answering the question whether they could be used as a nonpharmacological strategy to prevent, control, or ameliorate T2DM.

2. Materials and methods

2.1 Materials

Dulbecco's modified Eagle's medium (DMEM) containing 4.5 g L^{-1} glucose (25 mM), DMEM 1.0 g L^{-1} glucose (5.6 mM), DMEM no glucose, Ham's F-12 Nutrient Mix (F-12) 1.8 g L^{-1} glucose (10 mM), Roswell Park Memorial Institute medium (RPMI 1640) 2 g L^{-1} glucose (11.1 mM), fetal bovine serum, and phosphate-buffered saline (PBS, pH 7.4) and PrestoBlue Cell Viability Reagent were obtained from Life Technologies (Carlsbad, CA, USA). Antibiotics (penicillin and neomycin) were obtained from Serva (Heidelberg, Germany); amphotericin B, *c*POA, *t*POA, and a cyclic AMP ELISA Kit from Cayman

Chemical Company (Ann Arbor, MI, USA). A GeneMatrix Universal RNA Purification Kit, DNAse, NG dART RT kit, and SG qPCR Master Mix were purchased from EURX Sp. z o.o. (Gdańsk, Poland). Primers for rt-qPCR were obtained from Genomed S.A. (Warszawa, Poland). Ethanol, HCl, D-glucose, KCl, NaCl, $MgCl_2{\cdot}6H_2O$, $CaCl_2{\cdot}2H_2O$, HEPES, β-mercaptoethanol, nicotinamide, sodium selenite, transferrin, Bradford Reagent, 3-isobutyl-1-methylxanthine (IBMX) and bovine serum albumin (BSA) were purchased from Merck KGaA (Darmstadt, Germany). A Screen QuestTM Fluo-8 No Wash Calcium Assay Kit was purchased from AAT Bioquest, Inc. (Sunnyvale, CA, USA). Specific antagonists of GPR40 (DC260126, presented as DC), GPR55 (CID16020046, presented as CID), and GPR120 (AH7614, presented as AH) were obtained from Tocris Bioscience (Ellisville, MS, USA). The GPR119 antagonist (given as C8) was kindly provided by Pfizer (Groton, CT, USA).[30] All antagonists were prepared as 10 mM stock solutions in DMSO and 2 μM working concentrations were applied. Fatty acids were solubilized in ethanol at 5 mM concentration and further diluted in PBS.

2.2 Cell culture

Cell cultures were grown in a specific cell line culture medium supplemented with antibiotics (1% penicillin/amphotericin B/neomycin) at 37 °C with 5% CO_2. The murine adherent insulinoma MIN6 cells were kindly donated by Prof. Peter Bergsten from Uppsala University, Uppsala, Sweden, with the consent of Dr Jun-ichi Miyazaki from Osaka University, Japan.[31] The cells were grown in DMEM containing 25 mM glucose, 10% fetal bovine serum, and supplemented with 50 μM β-mercaptoethanol. The human pancreatic β cell line EndoC-βH1[32] was purchased from Human Cell Design (Toulouse, France). Cells were cultured in 1% extracellular matrix (ECM)/2 μg ml^{-1} fibronectin-coated flask. Cell medium composition was based on DMEM (w/o glucose)/Ham's F12 (50%/50%) with the addition of 2% albumin from bovine serum fraction V, 5.5 μg ml^{-1} transferrin, 6.7 ng ml^{-1} sodium selenite, 10 mM nicotinamide, and 50 μM 2-mercaptoethanol.

2.3 Cell viability

MIN6 cells and EndoC-βH1 cells were seeded into 96-well plates (3×10^4 cells per well) in 100 μl of culture medium and grown for 24 h. Next, cells were incubated for 24 h, 48 h, or 72 h in serum-free culture media (without 10% FBS and 2% BSA in culture media for MIN6 and EndoC-βH1 cells, respectively) in the presence of studied compounds at final concentrations of 5 μM, 10 μM, 25 μM, 50 μM, or 100 μM. According to the manufacturer's instructions, cell viability was determined with the fluorescence measurement at F530/590 nm using a PrestoBlue Cell Viability Reagent. The obtained values were used to calculate cell viability as the percentage of untreated control cell viability.

2.4 Determination of the critical micelle concentration (CMC)

Stock solution and serial dilutions of *cis*- and *trans*-palmitoleic acid were prepared in ethanol and mixed with the assay buffer to a final concentration of 2% ethanol. Nile Red was dissolved in DMSO to a final concentration of 40 μM in assay tubes. Before experiments, DMEM and Ca5 buffer were preheated to 37 °C. The reaction solution consisting of DMEM or Ca5 buffer, fatty acid-ethanol solution, and Nile Red was prepared in glass test tubes. Subsequently, the solution was mixed, and incubated in the dark at 37 °C for 30 minutes and then fluorescence (excitation/emission = 530/620 nm) was measured.

2.5 Insulin secretion at low (2 mM) and high (20 mM) glucose concentrations

MIN6 cells and EndoC-βH1 cells were seeded into a 24-well plate at a density of 2×10^5 cells per well and cultured for 48 h. Cells were pre-incubated in calcium buffer Ca5 (25 mM HEPES, 6 mM KCl, 125 mM NaCl, 1.3 mM $CaCl_2{\cdot}2H_2O$, 1.2 mM $MgCl_2{\cdot}6H_2O$) with 2 mM glucose for 60 min at 37 °C. Next, the cells were incubated in the new portion of the same Ca5-2 mM glucose buffer for 30 min, supplemented with tested fatty acids applied at 10 or 25 μM concentration and/or receptor antagonists (DC, CID, C8, AH) applied at a concentration of 2 μM. The buffer supernatants were saved and the 0.1% BSA was added to the collected samples. The cells were further incubated in Ca5-20 mM glucose buffer for 30 min with the tested compounds. The buffer samples were collected again and the 0.1% BSA was added. Samples from low and high glucose were subjected to insulin secretion measurements *via* competitive ELISA.[33] To normalize insulin levels, cells were lysed with 0.1 M HCl and the protein content of respective cell lysates was determined using the Bradford protein assay.

2.6 Calcium flux measurements

MIN6 and EndoC-βH1 cells were seeded into 96 well plates at a density of 4×10^4 cells per well and cultured for 24 h. Subsequently, the culture medium was changed to Ca5 buffer with 2 mM or 20 mM glucose. According to the producer's protocol, the intracellular calcium concentration $[Ca^{2+}]_i$ was measured with a Screen QuestTM Fluo-8 No Wash Calcium Assay Kit. To observe potential membrane permeabilization caused by investigated compounds, propidium iodide (PI) at a final concentration of 1 μg ml^{-1} was added just before the experiment. Calcium flux and PI intercalation were measured after adding fatty acids at 10 or 25 μM concentration and/or GPCR antagonists (DC, CID, C8, AH) applied at a concentration of 2 μM by a change in fluorescence (excitation/emission = 490/520 nm and 535/617 nm, respectively). Fluorescence reads were corrected for background fluorescence. The MAX fluorescence was read from the real-time kinetics of $[Ca^{2+}]_i$ quantitative data and calculated using the GraphPad program, which selects the first maximum peak after the addition of the test compound for each measurement and then averages the result.

2.7 cAMP synthesis measurements

MIN6 and EndoC-βH1 cells were seeded into 6 well plates at a density of 2×10^6 cells per well and cultured for 48 h. Next, the

standard culture medium was substituted with Ca5 buffer with 2 mM glucose and the cells were incubated for 60 min at 37 °C. The buffer was changed to a new portion supplemented with 20 mM glucose. Fatty acids were added at 10 or 25 μM concentration and/or receptor antagonists (DC, CID, C8, AH) were applied at 2 μM concentration together with 1 mM IBMX. The cells were incubated for 30 min at 37 °C. Accumulated cAMP was measured in cell lysates with the cyclic AMP ELISA Kit, according to the manufacturer's protocol and normalized to the protein content of respective cell lysates using the Bradford Protein Assay.

2.8 RNA isolation and quantitative reverse transcription PCR analysis

MIN6 and EndoC-βH1 cells were seeded into 6 well plates at a density of 2×10^6 cells per well and cultured for 24 h. Then, the culture medium was removed and cells were washed with PBS buffer. RNA was extracted and purified with a GeneMatrix Universal RNA Purification Kit protocol (with DNAse treatment). The purity and concentration of isolated RNA were checked with absorbance reads. RNA samples were reverse transcribed to cDNA with an NG dART RT kit protocol. RT-qPCR was carried out using an SG qPCR Master Mix protocol and CFX96 Touch Real-Time PCR Detection System (BioRad, USA). The sequences of specific primers were designed using the NCBI's Primer-BLAST software (National Center for Biotechnology Information) based on receptors' sequences from the GenBank database. Constitutively expressed *Actβ* or *GAPDH* genes were selected as endogenous controls to correct potential variation in RNA loading. The levels of receptor expression were normalized to the expressions of the housekeeping gene according to the $2^{-\Delta Ct}$ method.

The sequences of primers used in the study.

Gene symbol	Forward primer	Reverse primer	Accession no.
Primers for mouse gene expression detection (applied in MIN6 samples)			
Actβ	5′AAGAGCTATGAGCTGCCTGA3′	5′TACGGATGTCAACGTCACAC3′	NM_007393.5
Gpr40	5′TCTGCCTGGGGCCCTATAAT3′	5′TCCAGGACCTGTTCCCAAGT3′	NM_194057.3
Gpr55	5′AGCCTTCTGACTTGGACAGC3′	5′CCTCATCCCCTTCATACTGG3′	NM_001033290.2
Gpr119	5′CTTCTACTGTGACATGCTCAAGATTG3′	5′CCATGGCTCCTGCATGTTC3′	NM_181751.2
Gpr120	5′CTGGGGCTCATCTTTGTCGT3′	5′ACGACGAGCACTAGAGGGAT3′	NM_181748.2
Primers for human gene expression detection (applied in EndoC-βH1 samples)			
GAPDH	5′AGGGCTGCTTTTAACTCTGGT3′	5′CCCCACTTGATTTTGGAGGGA3′	NM_002046.7
GPR40	5′CTCCTTCGGCCTCTATGTGG3′	5′AGACCAGGCTAGGGGTGAGA3′	NM_005303.2
GPR55	5′GTTTCCATGGGAAAGTGGAA3′	5′GGAAGGAGACCACGAAGACA3′	NM_005683.4
GPR119	5′CTCCCTCATCATTGCTACTAA3′	5′ACAGCCAGATTCAAGGTG3′	NM_178471.2
GPR120	5′CCTGGAGAGATCTCGTGGGA3′	5′AGGAGGTGTTCCGAGGTCTG3′	NM_181745.4

2.9 Molecular modeling

2.9.1 Protein structure preparation. The structure of the human GPR40 receptor was imported from the Protein Data Bank (ID: 4PHU, resolved to 2.33 Å resolution in complex with TAK-875). The structures of GPR55, GPR119, and GPR120 were obtained from the AlphaFold2 database (**https://alphafold.ebi.ac.uk/**) using IDs: Q9Y2T6, Q8TDV5, and Q5NUL3, respectively. The structures of receptors, including 1-palmitoyl-2-oleoyl-*sn-glycero*-3-phosphatidylcholine/1-palmitoyl-2-oleoyl-*sn-glycero*-3-phosphatidylglycerol/cholesterol membrane, were prepared with a web-based CHARMM-GUI tool.[34] The spatial structures of receptors incorporated in the membranes are presented in ESI Fig. 1.†

2.9.2 Molecular docking. Blind docking was conducted using GNINA1.0 docking software[35] with the whole structure included for each of the four receptors with their membranes. Docking of each ligand was performed three times, with maximum exhaustiveness (100), at an energy of 10 kcal mol^{-1}, and CNN scoring set to refinement. Fourteen CPUs were employed to conduct these calculations.

Conventional molecular dynamics. All preparation steps, simulations and trajectory postprocessing were performed using AMBER20 software.[36] Complexes obtained through molecular docking were subjected to preparation using tLeap, where ff19SB,[37] OPC,[38] lipid17,[39] and gaff2[40] force fields were defined for protein, water, lipid membrane, and ligands, respectively. Partial charges of ligands were calculated at the RESP[41,42] level of theory and inputs were generated using an antechamber.[42] The conventional molecular dynamics (MD) simulation procedure applied was described in the previous study.[25]

To explicitly compare *c*POA and *t*POA, a Thermodynamic Integration (TI) analysis, based on a transformation of one substrate into another within selected "windows", was applied. Such a method is based on calculating the difference in energy between the protein–ligand system, in which one ligand turns into another one, and the protein-free system, where ligands contained only within a box of water undergo transformation. Preparation of calculations consisted of selecting "softcore" atoms that will be substituted and "core" atoms, which will remain unchanged throughout the whole analysis. Exemplification of softcore and core atoms can be found in ESI Fig. 2.†

Ligand–receptor complexes for TI analysis were prepared by removing them from the membranes, as membranes are not necessary and increase the computational cost of calculation. Initial minimization, heating, and equilibration of the systems (20 000 steps, 10 000 of which in conjugant gradient, heating for 100 ps and 20 ns of equilibration, with a timestep of 1 fs). Free energy simulations in TI were based on the transformation of the molecules using a set of 12 steps (lambdas), set

exponentially from 0 to 1 excluding boundary values, as suggested by ref. 43 and the calculation of the van der Waals force contribution. Each "window" consisted of a 5 ns production simulation, during which the algorithm calculated the binding energy differences using a timestep of 1 fs. It is worth mentioning that in TI the ligands in the water box were calculated solely using CPUs, while ligand–receptor complexes were calculated using GPUs.

2.9.3 Computational environment. All the images presented in the study were prepared using an open-source version of PyMOL. Calculations contained within the manuscript were performed on computational clusters (PL-GRID, and in-house using a workstation equipped with Intel® Core™ i9-9900KF CPU @ 3.60 GHz × 16 with 32 GB @ 2666 MHz with GeForce RTX 2070 SUPER/PCIe/SSE2 on the Ubuntu 20.04 Focal Fossa.

2.10 Statistical analysis

The biological results are presented as means of 3–6 repeated experiments ± SEM. Data were compared using one-way ANOVA with Bonferroni *post hoc* test or two-way ANOVA for cell viability experiments and insulin secretion under low and high glucose conditions. The $p < 0.05$ was considered statistically significant. To exclude the impact of fatty acids on the solvents all results were compared to the cells where only the appropriate volume of this solvent was added (control cells). Data analysis and graph design were performed with GraphPad Prism v. 8.3 (GraphPad Software, La Jolla, CA, USA).

3. Results

3.1 Effect of *cis* and *trans* isomers of palmitoleic acid on the viability of pancreatic β cells

To recapitulate the vulnerability of pancreatic β cells of human and murine origin to isomers of palmitoleate, we first exposed MIN6 and EndoC-βH1 to various concentrations of either *c*POA or *t*POA (5–100 μM). Exposure to both fatty acids decreased cell viability in a concentration-dependent manner (Fig. 1). The cytotoxic effect of *c*POA, however, was more profound as compared with *t*POA. For example, after 24 h of incubation, the inhibitory effect of *c*POA was significant ($P < 0.05$) at 25 μM in the case of MIN6 and 50 μM in the case of EndoC-βH1. In comparison, the growth of the EndoC-βH1 cell line was reduced at 100 μM *t*POA after being treated for 24 h. Overall, the addition of 10 μM concentration of both structural isomers of palmitoleic acid was determined to be appropriate as it was non-toxic and was employed in the subsequent tests.

However, since *c*POA reduced the viability of cell lines under study at lower concentrations than *t*POA, we aimed to investigate the aggregation behaviors of POA isomers. Fatty acids can form micelles or micelle-like structures despite their long hydrophobic moiety due to the carboxyl functional group that improves water solubility.[44] The formation of aggregations reduces the system's free energy by removing hydrophobic fragments from the aqueous environment. The concentration at which micelle formation is first seen in the solution is called the critical micelle concentration (CMC).[45] Since the loss of cell viability and cell lysis strictly depend on CMC values,[46] we established the potency of

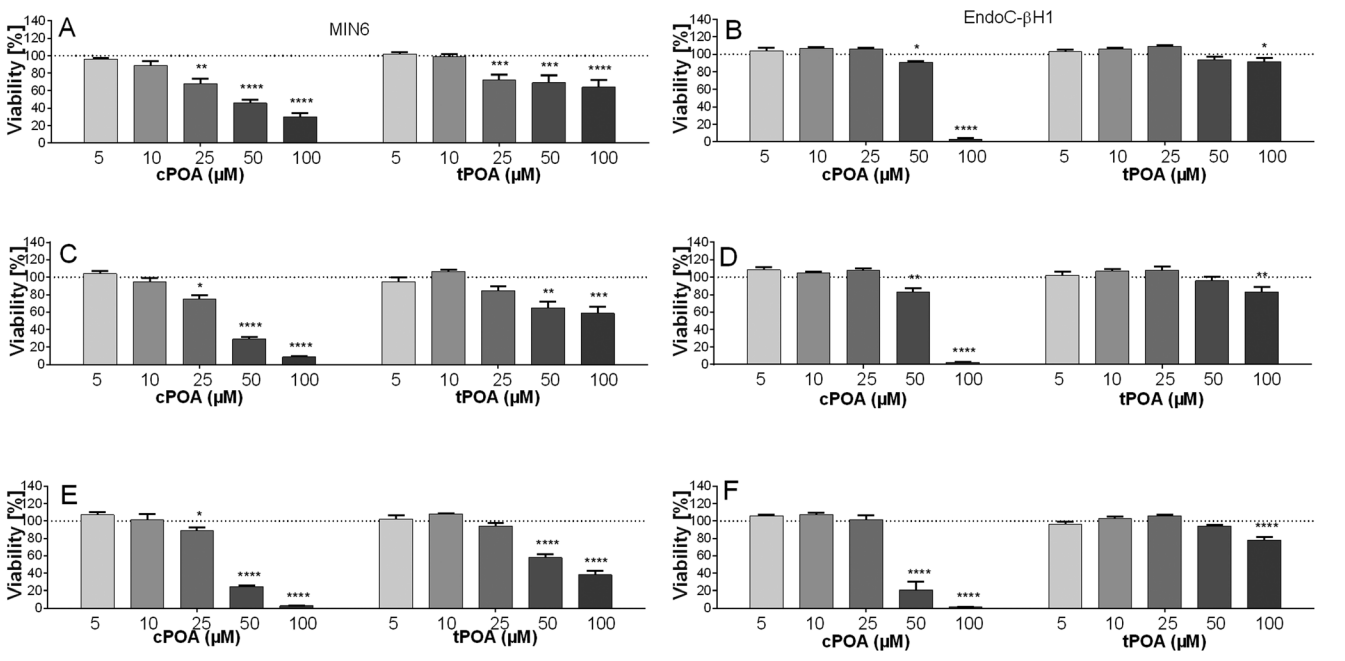

Fig. 1 The effect of *cis* and *trans* isomers of palmitoleic acid on the viability of MIN6 (A, C and E) and EndoC-βH1 (B, D and F) after 24 h (A and B), 48 h (C and D), and 72 h (E and F) of treatment in the concentration range of 5–100 μM. The results are expressed as % of living cells after treatment of control cells with a respective compound solvent. The bars represent the means ± SEM, $n = 3–4$ independent experiments. ****$p < 0.0001$, ***$p < 0.001$, ***$p < 0.01$, and *$p < 0.05$ *vs.* control.

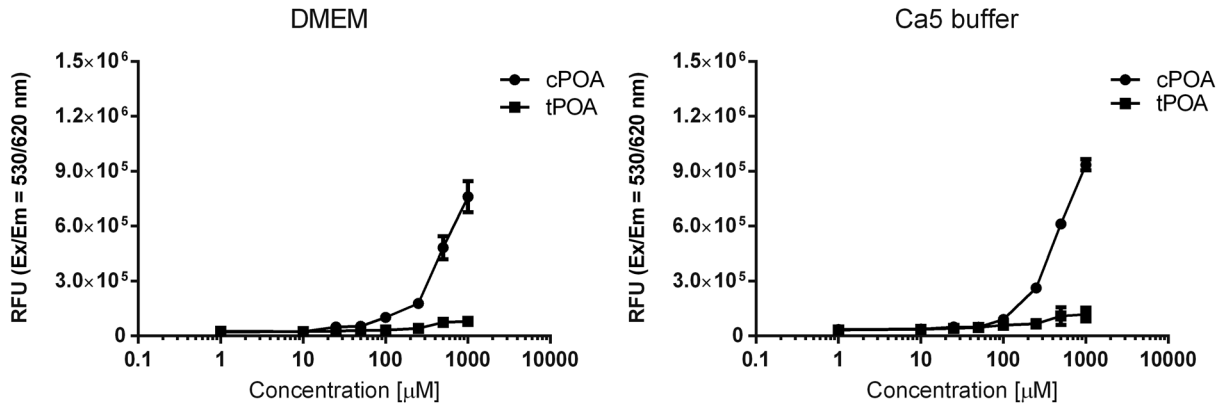

Fig. 2 The dependence of the Nile Red fluorescence intensity on the logarithmic concentration of POA isomers in DMEM culture medium and Ca5 buffer. The mixture of fatty acids and medium/buffer was prepared in low adhesive containers which have been shaken for 30 minutes and covered from light. The fluorescence intensity of Nile Red was measured immediately after incubation at an excitation wavelength of 530 nm and an emission wavelength of 620 nm. Data are presented as means ± SEM, n = 4–8 independent repeats.

POA isomers to create micelle-like structures with a Nile Red lipophilic fluorescent probe. The Nile Red method relies on a sharp change in the fluorescence intensity in a lipid-rich environment when the dye binds to micelles.[44]

The Nile Red fluorescence intensities of the samples were measured after exposure to various concentrations of free fatty acids in aqueous solutions such as DMEM culture medium and Ca5 buffer (Fig. 2), the latter used during insulin secretion experiments. The fluorescence showed no significant differences when the concentrations of *c*POA and *t*POA were low (1–10 μM), indicating that they could not form aggregates. However, when the concentration of *c*POA was gradually increased, the Nile Red assays revealed sharp fluorescence intensity changes starting at 100 μM. This critical micelle concentration showed that *c*POA could form hydrophobic domains. In the case of *t*POA, the rise was not so substantial. Moreover, the observed higher fluorescence intensity of *c*POA samples suggests the existence of higher micelle density as compared to *t*POA. Therefore, differences in the micelle formation of POA isomers may be responsible for the differences in their cytotoxicity and explain why *c*POA was more aggressive than *t*POA in MIN6 and EndoC-βH1 cells.

3.2 Both *c*POA and *t*POA potentiate insulin secretion in pancreatic murine and human β cells

In the next step, we tested whether *c*POA and *t*POA could increase insulin secretion at low and high glucose concentrations in clonal MIN6 and EndoC-βH1 pancreatic β cells. *c*POA and *t*POA applied at 10 μM concentration did not affect insulin secretion in murine MIN6 cells (Fig. 3A). However, adding 25 μM palmitoleate isomers improved glucose responsiveness in the MIN6 cell line (Fig. 3B). At the same time, both isomers used at 10 μM concentration promoted glucose-induced insulin secretion to a similar degree under 20 mM glucose conditions in EndoC-βH1 cells (Fig. 3C). Under 2 mM glucose, the effect was less profound (Fig. 3C). We also tested how prolonged exposure (24 h) of cells influence GSIS itself and the activity of *cis*- and *trans*-POA and compared those result to acute treatment (1.5 h). Basal insulin secretion did not change significantly after a 24 h-incubation period in both pancreatic β cell lines. As compared with acute treatment, incubation of MIN6 cells with 25 μM *c*POA and *t*POA caused a slight rise in the level of released insulin (ESI Fig. 2A and B†), similar to EndoC-βH1 treated with 10 μM POA isomers (ESI Fig. 2C and D†). Therefore, chronic treatment with POA isomers does not have a harmful effect on the potential of cells to induce insulin secretion. In contrast, long-term stimulation with *c*POA and *t*POA may be advantageous rather than deleterious for the β cells in terms of GSIS.

To understand the mechanism underlying the potent insulin secretagogue activity of *c*POA and *t*POA, we used the ability of selective antagonists to block GPR40, GPR55, GPR119, and GPR120 receptors. Four fatty acid lipid-sensing GPCRs under the study are preferentially expressed on β cells of pancreatic islets.[29] We have previously demonstrated the expression of *Gpr40*, *Gpr55*, and *Gpr119* in MIN6 cells.[47] Here, we have detected all transcripts in both cell lines studied. In MIN6 cells *Gpr40* mRNA was the most abundant, followed by *Gpr120*. *Gpr55* and *Gpr119* were detected at very low levels (Fig. 3D). In turn, in EndoC-βH1 cells *GPR40*, *GPR119*, and *GPR55* were expressed with a similarly high degree (Fig. 3E).

*c*POA was shown previously to activate GPR120 in HEK 293 cells stably expressing GPR120.[48] We found in this study that the promotion of insulin secretion by *c*POA and *t*POA was not only GPR120-dependent. DC260126, CID16020046, and C8, selective antagonists of GPR40, GPR55, and GPR119, also partially blocked the response evoked by 25 μM POA isomers in MIN6 cells (Fig. 3F) and 10 μM POA isomers in EndoC-βH1 (Fig. 3G).

3.3 Effect of *cis* and *trans* isomers of palmitoleic acid in Ca^{2+} signaling in pancreatic β cells

GPR40,[49] GPR55,[50] GPR119,[51] and GPR120 [52] are considered to be Gq-coupled receptors promoting Ca^{2+} mobilization. When

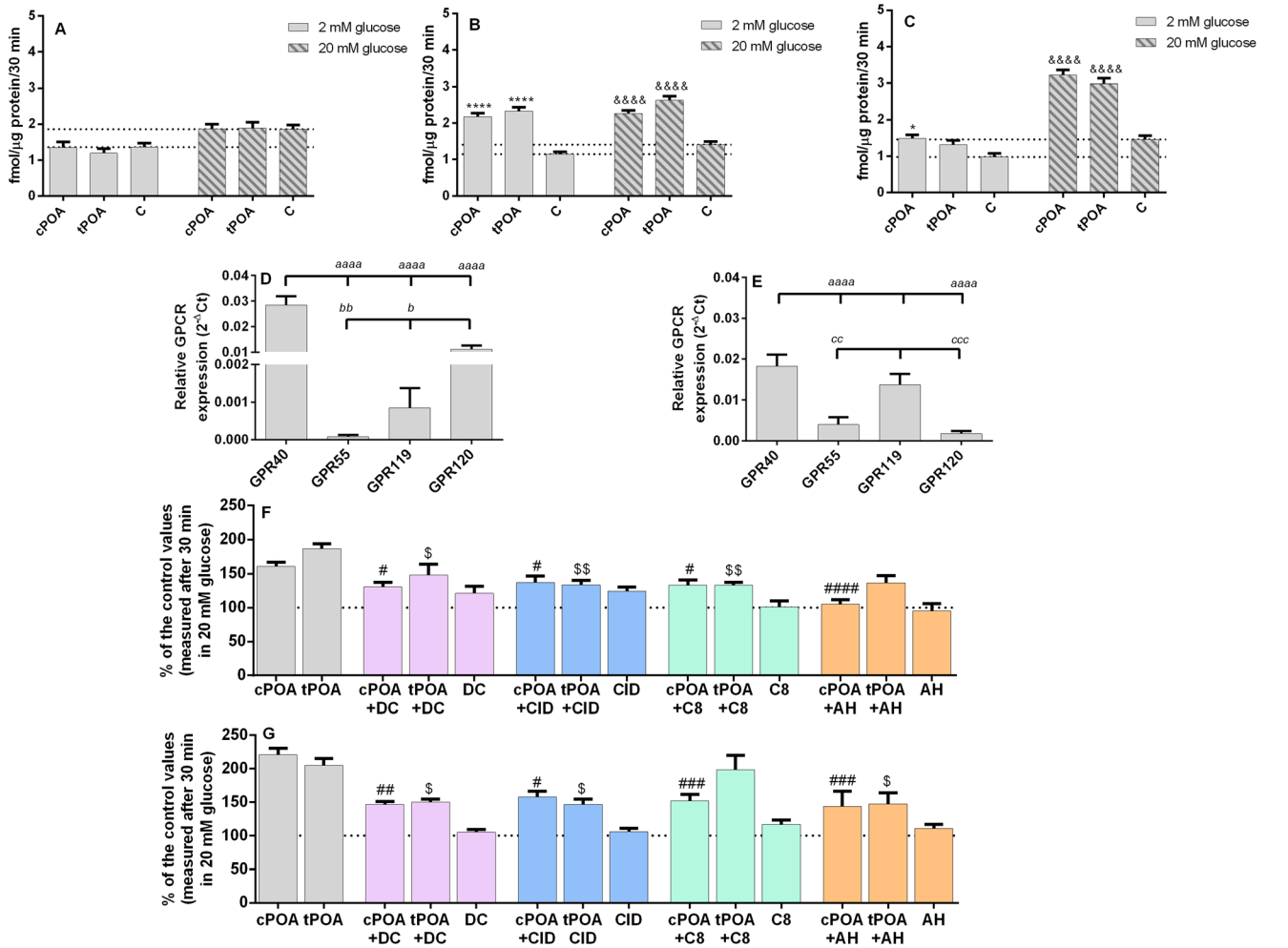

Fig. 3 *cis* and *trans* isomers of palmitoleic stimulate insulin secretion and *c*POA and *t*POA-enhanced GSIS is partially abrogated by GPR40, GPR55, GPR119, and GPR120 receptor antagonists. (A) MIN6 treated with *c*POA and *t*POA (10 µM); (B) MIN6 treated with *c*POA and *t*POA (25 µM); (C) EndoC-βH1 treated with *c*POA and *t*POA (10 µM); (D) *Gpr40*, *Gpr55*, *Gpr119*, and *Gpr120* expression patterns in MIN6 cells normalized to a housekeeping gene (*Actβ*); (E) *GPR40*, *GPR55*, *GPR119*, and *GRP120* expression patterns in EndoC-βH1 cells normalized to a housekeeping gene (*GAPDH*); (F) MIN6 treated with *c*POA and *t*POA (25 µM) + DC260126, CID16020046, C8, or AH7614 (2 µM) in 20 mM glucose; (G) EndoC-βH1 treated with *c*POA and *t*POA (10 µM) + DC260126, CID16020046, C8, or AH7614 (2 µM) in 20 mM glucose. The bars represent the means ± SEM, n = 3–5 independent experiments. Data in (F) and (G) are presented as percentages of control values. **** $p < 0.0001$, * $p < 0.05$ *vs.* 2 mM glucose control; &&&& $p < 0.0001$, && $p < 0.01$ *vs.* 20 mM glucose control; #### $p < 0.0001$, ### $p < 0.001$, ## $p < 0.01$, # $p < 0.05$ *vs.* *c*POA; $$ $p < 0.01$, $ $p < 0.05$ *vs.* *t*POA; *aaaa* $p < 0.0001$ *vs.* GPR40; *bb* $p < 0.01$, *b* $p < 0.05$ *vs.* GPR120; *ccc* $p < 0.001$, *cc* $p < 0.01$ *vs.* GPR119.

ligands bind to those receptors, the G subunit is activated by GDP/GTP exchange and separates from the trimeric G protein. Subsequent binding to phospholipase C (PLC) increases intracellular inositol triphosphate (IP_3) and diacylglycerol (DAG) levels through the hydrolysis of phosphatidylinositol 4,5-bisphosphate (PIP_2).[29] Thus, we investigated calcium signaling mediated by POA isomers in pancreatic MIN6 and EndoC-βH1 cell lines since the release of Ca^{2+} from the endoplasmic reticulum is mediated by IP_3. Potential membrane permeabilization was monitored with propidium iodide staining (ESI Fig. 3†). A final concentration of 10 µM *c*POA induced a rapid and transient rise of intracellular calcium concentration in EndoC-βH1 cells (Fig. 4D), while no such response was seen in MIN6 cells (Fig. 4A). Following GSIS results, the addition of 25 µM *c*POA resulted in the rise of intracellular calcium concentration in the MIN6 cell line (Fig. 4B). The responses evoked by *t*POA were similar to *c*POA in MIN6 cells (Fig. 4B) and lower in EndoC-βH1 cells (Fig. 4C). The size of these responses was quantified by calculation of the maximal fluorescence (excitation/emission = 490/520 nm) corresponding to the peak height (Fig. 4C and E).

To find out whether intracellular Ca^{2+} mobilization was GPCR-dependent, we have pre-incubated EndoC-βH1 cells with DC260126, CID16020046, C8, and AH7614 after which the palmitoleate-mediated calcium response was measured. As shown in Fig. 4F and H, the *c*POA response was partially reduced. Administration of antagonists in EndoC-βH1

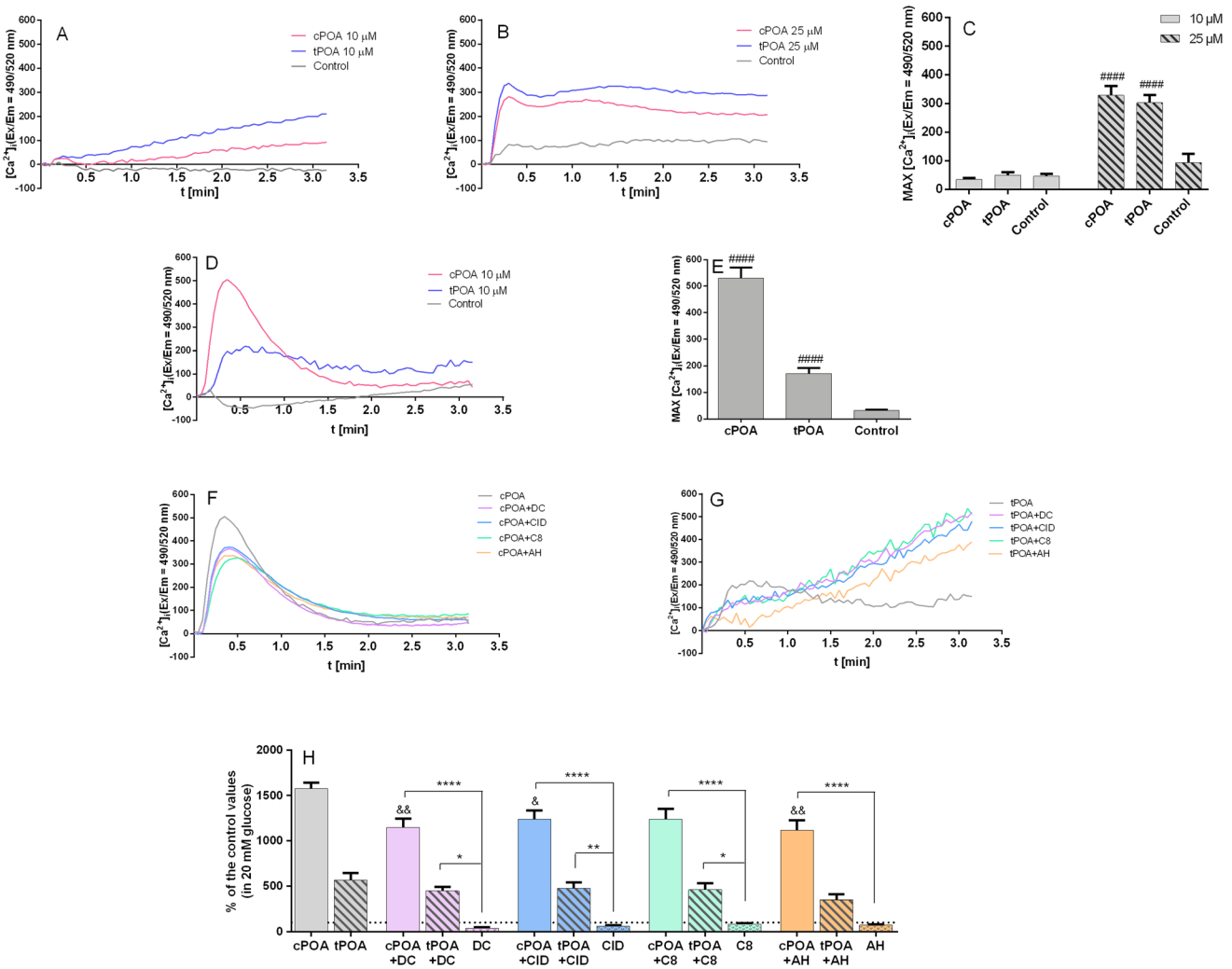

Fig. 4 Intracellular Ca^{2+} mobilization in MIN6 (A–C) and EndoC-βH1 (D–H) cells triggered by *cis* and *trans* isomers of palmitoleic acid at 20 mM glucose. MIN6 were treated with 10 µM (A and C) or with 25 µM *c*POA and *t*POA (B and C); EndoC-βH1 were treated with 10 µM *c*POA and *t*POA alone (D and E) or pretreated with DC260126, CID16020046, C8, or AH7614 used at a concentration of 2 µM (F–H). The results are presented as the average of the real-time kinetics of $[Ca^{2+}]_i$ changes inside the cell during 3 min-time monitoring (A, B, D, F and G) as well as MAX fluorescence (C, E and H). The bars represent the means ± SEM, n = 3–6 independent experiments. Data in (H) are presented as the percentage of control values. ####$p < 0.0001$ *vs.* respective control cells; &&$p < 0.01$, &$p < 0.05$ *vs. c*POA; ****$p < 0.0001$, **$p < 0.01$, and *$p < 0.05$ *vs.* respective antagonist.

cells resulted in the inhibition of *c*POA-mediated calcium responses. However, *t*POA itself was less potent (Fig. 4G and H).

3.4 Effect of *cis* and *trans* isomers of palmitoleic acid on the intracellular cAMP accumulation in pancreatic β cells

Based on the knowledge that GPCRs often signal through more than one pathway and that Gs signaling very efficiently stimulates insulin release,[29] we decided to study the effect of palmitoleate isomers with respect to the stimulation of cAMP accumulation. We measured cAMP synthesis in MIN6 and EndoC-βH1 pancreatic β cells after 30 min of incubation with POA isomers in the presence of 20 mM glucose and 1 mM IBMX. We used *c*POA and *t*POA at concentrations that effectively stimulated GSIS, namely 25 µM for MIN6 cells and 10 µM *c*POA for the EndoC-βH1 cell line. *c*POA did not cause significant changes in cAMP accumulation compared to unstimulated control cells in both cell lines (Fig. 5A and B). Interestingly, *t*POA caused a 1.7-fold increase in EndoC-βH1 cells (Fig. 5B). Administration of *t*POA in MIN6 also augmented the cAMP concentration, however, the rise was only about 25% compared to control cells (Fig. 5A). As in the case of calcium signaling, we decided to check the possible correlation between the increase in cAMP accumulation caused by *t*POA and the activation of G protein-coupled receptors. We found that cAMP responses elicited by *t*POA in the EndoC-βH1 cells were linked to the GPR40 receptor to the greatest extent (Fig. 5C). Therefore, we show here for the first time that *t*POA can activate at least GPR40 and signal not only through Gq as observed with the endogenous lipid ligands but also in a ligand-biased way through Gs.

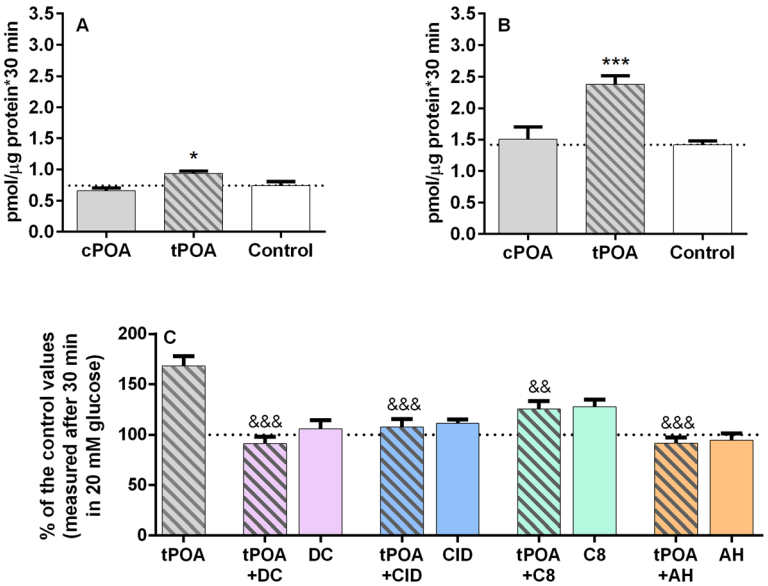

Fig. 5 Intracellular cAMP accumulation in MIN6 (A) and EndoC-βH1 (B) cells triggered by *cis* and *trans* isomers of palmitoleic acid at 20 mM glucose. MIN6 and EndoC-βH1 were treated with 25 μM and 10 μM *c*POA and *t*POA, respectively. EndoC-βH1 cells were also pretreated with DC260126, CID16020046, C8, or AH7614 used at a concentration of 2 μM and then incubated with 10 μM *t*POA (C). The bars represent the means ± SEM, $n = 3$ independent experiments. Data in (C) are presented as percentages of control values. ***$p < 0.001$, *$p < 0.05$ *vs.* respective control cells; &&&$p < 0.001$, &&$p < 0.01$ *vs.* *t*POA.

3.5 Molecular docking, molecular dynamics, and thermodynamic integration analysis of the binding affinity of the *cis* and *trans* isomers of palmitoleic acid towards selected receptors

The results of *in vitro* experiments suggest that both *t*POA and *c*POA exhibit activity towards GPR40, GPR55, GPR119, and GPR120 receptors. As an additional validation method, a detailed *in silico* analysis was also applied here. The high-resolution X-ray structure of GPR40 in complex with fasiglifam (TAK-875), an orally available GPR40 agonist activating the Gq signaling pathway[53] and structures of GPR55, GPR119, and GPR120, obtained from the AlphaFold2 database (**https://alphafold.ebi.ac.uk/**), were used for computational analysis of potential binding affinities of palmitoleate isomers. Structures of investigated receptors were embodied in the lipid membrane, consisting of neutral phosphatidylcholine lipids, negatively charged phosphatidylglycerol lipids, and cholesterol. Each receptor was subjected to equilibration in the membrane due to its importance for appropriate receptor function.[54] Only for the thermodynamic integration the proteins were removed from the membrane, as the direct vicinity of ligands is important.

To ensure the validity of conducted calculations, conventional molecular dynamics simulations were subjected to analysis in terms of protein radius of gyration (R_g, ESI Fig. 4†), the solvent-accessible surface area of ligands (SASA, ESI Fig. 5†), root-mean square deviation of ligand position (ESI Fig. 6†) and protein Cα atoms (ESI Fig. 7†). On the other hand, due to the nature of thermodynamic integration analysis, we assessed the quality of simulation preparation through system density equilibration (ESI Fig. 8†). The results of the investigation analysis indicate some stabilization of each ligand–receptor complex. The radius of gyration and protein Cα atoms remained stable, with some fluctuations derived from the displacement of loops not embraced by the membrane. Systems were equilibrated before thermodynamic integration, with negligible density fluctuations.

All employed methods indicate a very similar affinity of both ligands towards the selected receptors, regardless of the resolution of the method. In terms of the *in silico* study, only thermodynamic integration could indicate some differences between the binding affinities of selected isomers. TI indicates the slightly higher affinity of *t*POA towards GPR40, GPR119, and GPR120 receptors. It suggests that the differences between the binding energies of both ligands are subtle. In the case of GPR40, the difference is notable (*t*POA binds to the receptor with a lower energy of −9 kcal mol^{-1} than *c*POA). In the cases of GPR119 and GPR120, the estimated affinity is very similar, albeit indicating a slight preference toward *t*POA (ESI Fig. 9†). A summary of all calculations is presented in Table 1.

As one may notice, the values for all molecular dockings are very similar with moderate binding energy. Molecular dynamics, however, show a somewhat higher binding affinity of both POA isomers towards the GPR40 receptor, but these fatty acids can potentially activate all selected receptors. Thermodynamic Integration indicates that *t*POA is a ligand favored by GPR40, 119, and 120 receptors with the strongest tendency for GPR40. The GPR55 does not differentiate between *cis*- and *trans*-POA according to TI analysis. Notably,

Table 1 Binding affinities of *c*POA and *t*POA towards GPR40, GPR55, GRP119, and GPR120

Receptor	Ligand	Molecular docking binding energy [kcal mol^{-1}]	Molecular dynamics binding energy [kcal mol^{-1}]	TI $\Delta\Delta G$ transformation [kcal mol^{-1}]	Ligand RMSD	SASA [A^2]
GPR40	*c*POA	−6.7 ± 0.5	−77 ± 5	−9 ± 0.7	1.87 ± 0.25	78 ± 25
	*t*POA	−6.7 ± 0.5	−74 ± 5		2.02 ± 0.39	74 ± 28
GPR55	*c*POA	−7.4 ± 0.4	−48 ± 7	0.1 ± 1.4	1.99 ± 0.23	191 ± 36
	*t*POA	−7.2 ± 0.5	−42 ± 6		2.09 ± 0.18	188 ± 42
GPR119	*c*POA	−7.3 ± 0.2	−49 ± 11	−1.7 ± 0.7	2.24 ± 0.18	30 ± 21
	*t*POA	−7.3 ± 0.3	−45 ± 11		2.01 ± 0.27	55 ± 24
GPR120	*c*POA	−7.2 ± 0.2	−41 ± 7	−1.9 ± 0.3	2.21 ± 0.21	87 ± 31
	*t*POA	−7.3 ± 0.2	−40 ± 6		2.07 ± 0.21	132 ± 37

there are no significant differences considering RMSD and SASA between selected ligands. Moreover, both remained stable during all simulations. The only observable difference between ligands can be found in exposition to the solvent – in cases of GPR119 and GPR120 *t*POA is less buried within the protein (Fig. 6), thereby increasing the probability of diffusion from the receptor. However, such a situation did not occur throughout the simulation, as the ligand RMSD remained stable.

Several residues within the GPR40-binding pocket were identified previously to contribute to binding linoleic acid and synthetic small molecule agonists. Arg183, Asn244, and Arg258 were shown to bind linoleic acid and GW9508 synthetic agonist by their carboxyl groups while His86, Tyr91, and His137 created hydrophobic interactions with GW9508 but not with linoleic acid. It was also suggested that Tyr12, Tyr91, His137, and Leu186 are essential for receptor activation.[55] The crystal structure of the GPR40 complex with partial agonists, TAK-875 and MK-8666, confirmed the importance of Tyr91, Arg183, and Arg258 in binding.[53] Additionally, Tyr240 was revealed as a crucial amino acid residue in an allosteric site.[56] For natural ligands of GPR40, this site was responsible for binding a carboxyl residue. In our study, both palmitoleic acid isomers were trapped in the polar pocket of Arg183, Tyr240, and Arg258 to create hydrogen bonds with the carboxyl group (distance less than 2.1 Å). The GPR40-*c*POA model reveals hydrophobic interactions with Val84, Phe87, Leu135, Leu138, Phe142, Trp174, and Leu186. The GPR40-*t*POA model shows a similar space, but the double bond of *t*POA straightens the molecule, changing some interactions with receptor active site residues (same Phe87, Leu135, Leu138, and Leu186 but also Val141, Ala146, and Leu158) (Fig. 6). This may explain the difference in GPR40 activation pathways. Hauge *et al.* described the combined signaling of GPR40 *via* Gq and Gs pathways. They show that the binding site for Gq and/or Gs agonists are nearly the same.[49]

We employed models from the AlphaFold2 database to analyze interactions between POA isomers and GPR55, GPR119, and GPR120 receptors. Previous homology modeling studies of GPR55 with natural ligands demonstrated that Lys80, Tyr101, Val242, and Phe239 (in the case of cannabidiol) or Lys80, Ser84, Phe102, Phe239, Val242, and Gln271 (for 2-arachidonoyl-lysophosphatidylcholine) stabilize the bound agonists. Carbonyl moieties of 2-arachidonoyl glycerol bind *via* hydrogen bonds with Lys80 while the long hydrophobic tail has to be flanked by Tyr101, Phe102, Val242, and Phe246.[57] Lys80, Glu98, Tyr101, and His170 were also identified as crucial residues for activation by lysophosphatidylinositol and the ML184 synthetic agonist.[58] In our model, the carboxyl group of both fatty acids was attracted by Gln249 and Ser267 forming hydrogen bonds. For *t*POA, an additional hydrogen bond with Arg253 was observed. The middle part of both compounds created similar hydrophobic interactions with Phe102, Phe246, and Leu270. *c*POA created hydrophobic interactions with Phe156, Phe159, and Leu185 while *t*POA with Trp177 and Phe182 (Fig. 6).

Based on the homology model of GPR119 with natural and synthetic agonists (lysophosphatidylcholine, oleoylethanolamide, and 2-methoxy-lysophosphatidylcholine) His162, Pro163, Ser170, Thr244, Gly245, Gln248, Val249, and Arg262 were identified in a binding pocket.[59] Guided mutation confirmed the crucial role of previously mentioned residues for oleoylethanolamide, adding Arg81, Thr86 and Ser170.[60] The polar group of *cis*- and *trans*-palmitoleic acids in complex with GPR119 binds with Thr86 and Trp265. However, *c*POA created significantly fewer interactions than *t*POA. More linear *c*POA created hydrophobic interactions with Ala89, Val132, Leu169, and Trp238, while more clustered *t*POA except Leu169 and Trp238 connected with Ala90, Val93, Leu94, Phe174, and Ala177 (Fig. 6).

In the GPR120-POA complex, *c*POA recruits a different group of amino acids than *t*POA. The polar carboxyl moiety of *t*POA did not form any visible interactions with GPR120 while Arg24 attracted this group in *c*POA *via* hydrogen bonds. Additionally, *c*POA was stabilized by hydrophilic interactions with Arg22 and hydrophobic interactions with Phe25, Phe27, and Ile287. In our model, *t*POA created only hydrophobic interactions with GPR120 by Phe25, Phe27, Phe88, Leu173, Ile287, and Phe303 (Fig. 6). Binding interactions between α-linoleic acid and GPR120 were also published. A guanidine ring of Arg99, which binds the carboxyl group of an α-linoleic acid, plays a crucial role.[61] Furthermore, α-linoleic acid displayed additional interaction with Phe88, Trp104, Phe115, Trp207, Phe211, Trp277, Phe303, Phe304, and Thr310.[62] Glu249 seems to be essential for phytosphingosine binding but has minor importance in interactions with α-linolenic acid.[63]

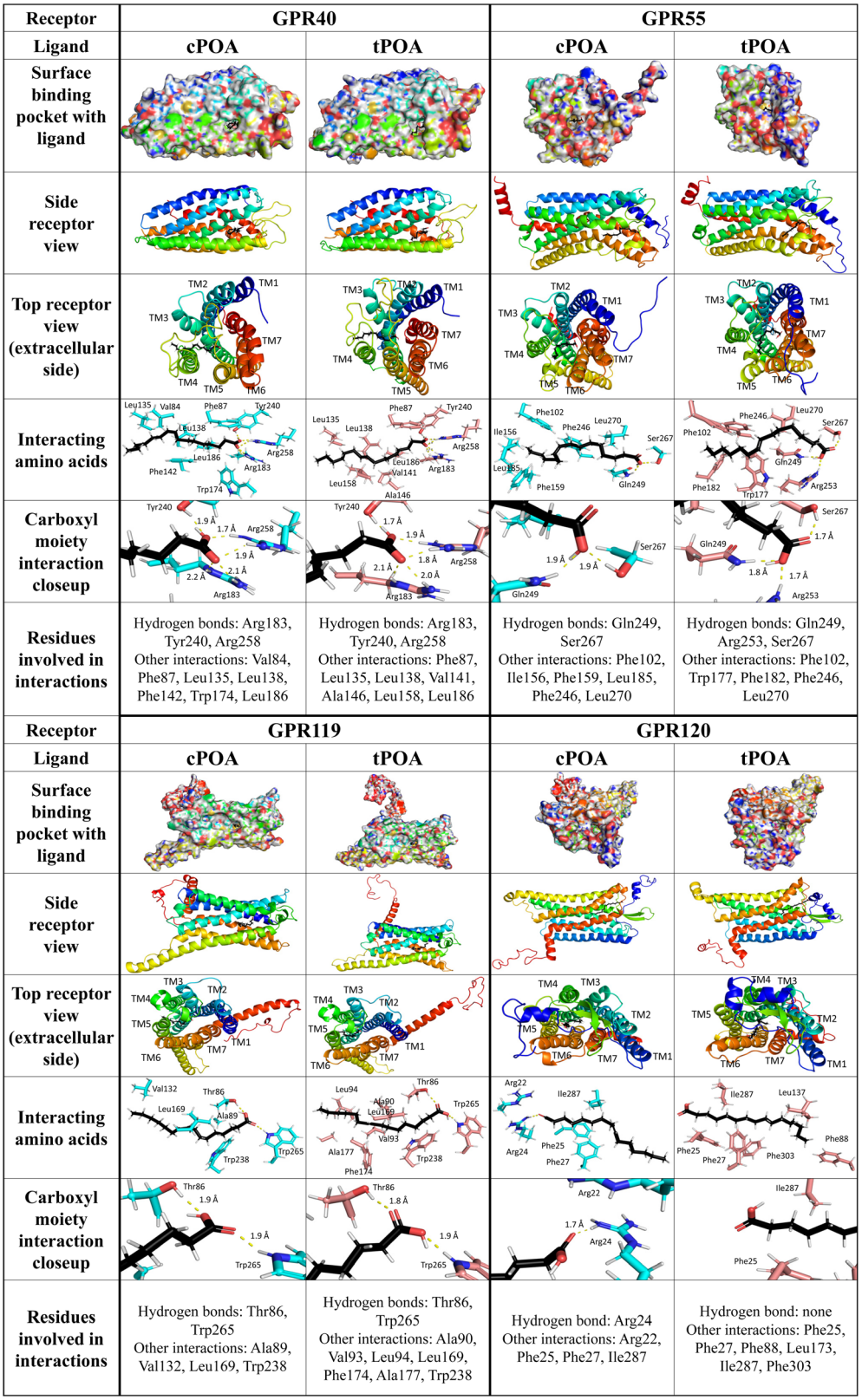

Fig. 6 Spatial orientation of *cis*- and *trans*-palmitoleic acid in complex with GPR40, GPR55, GPR119, and GPR120. Presentation of a biding pocket with a receptor surface, ligand localization (side and top view), the nearest neighborhood of the bonded ligand, a close-up of the polar carboxyl moiety of the ligand and the list of all detected interactions. Hydrogen bonds were indicated with a yellow dotted line.

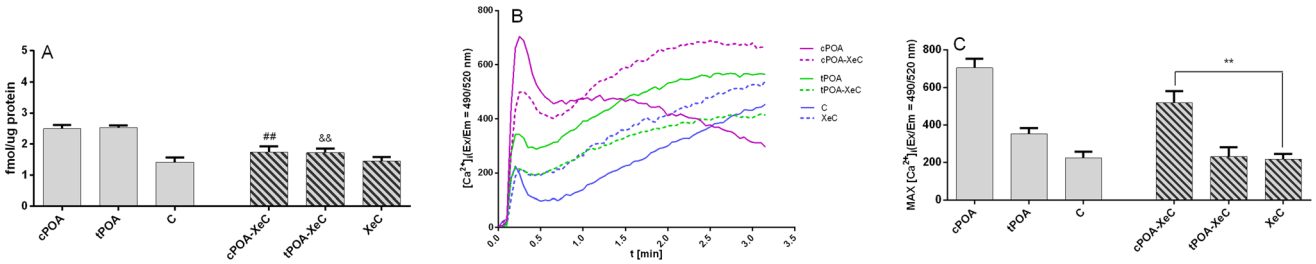

Fig. 7 Insulin secretion (A) and mobilization of intracellular Ca^{2+} (B and C) in MIN6 cells enhanced by the *cis* and *trans* isomers of palmitoleic acid at 20 mM glucose is partially abrogated by Xestospongin C (XeC), the IP_3 receptor antagonist. MIN6 were treated with 25 μM *c*POA and *t*POA alone or pretreated with XeC used at a concentration of 2 μM. The results are presented as the real-time kinetics of $[Ca^{2+}]_i$ changes inside the cell during 3 min-time monitoring (B) as well as MAX fluorescence (C). The bars represent the means ± SEM, n = 3 independent experiments. &&p < 0.01 *vs.* *c*POA; ##p < 0.01 *vs.* *t*POA; **p < 0.01 *vs.* XeC.

Since the GPR40-*c*POA and GPR40-*t*POA complexes displayed the most favorable binding energy and active site architecture, we decided to additionally confirm the interaction of POA through GPR40. Recently, Usui *et al.* reported that IP_3 receptor 1 (IP_3R1) plays an important role in the initiation of store-operated Ca^{2+} entry (SOCE) and subsequent GSIS stimulation by fasiglifam in MIN6 cells. The authors demonstrated the critical role of the IP_3R1/STIM1/Orai1 pathway in GPR40-mediated GSIS potentiation evoked by fasiglifam. At the same time, they showed that IP_3R1 was expressed in MIN6 cells.[64] We decided to employ Xestospongin C (XeC), a selective and membrane-permeable antagonist of the IP_3 receptor, since Xestospongin C was shown to inhibit fasiglifam-mediated GSIS potentiation in islets of C57BL/6 mice. Pretreatment of MIN6 cells with XeC abolished *c*POA- and *t*POA-mediated GSIS (Fig. 7A) as well as mobilization of intracellular Ca^{2+} (Fig. 7B and C).

4. Discussion

The literature on POA and health is inconsistent.[65] We sought to determine whether *cis*- and *trans*-POA isomers have similar biological effects on insulin secretion from human and murine β cell lines and on their transmembrane receptors, *e.g.*, GPR40, GPR55, GPR119, and GPR120 which were previously identified in mediating GSIS.

We found it reasonable to conduct comparative studies on cell lines from two species: human and mouse, especially since the results of the only animal study dealing with *t*POA and glucose homeostasis are contradictory to human trials.[18] Also, there are many differences between human islet cells and mouse models such as hormone secretion, innervation, angiogenesis, cell type composition, islet-enriched transcription factor distribution, mitotic stimulation, stress response signaling, or lipid droplet accumulation.[66]

Our experiments demonstrated the stimulatory effect of *c*POA and *t*POA on insulin release in MIN6 and EndoC-βH1 cells. The level of stimulation was comparable for both isomers. However, differences between the mouse and human cell lines were revealed. We showed that *c*POA and *t*POA induced insulin secretion in human EndoC-βH1 cells but did not affect insulin secretion in murine MIN6 cells applied at the same (10 μM) concentration. Increasing the concentration of POA isomers to 25 μM improved the responsiveness of the MIN6 cell line suggesting that the mouse line is less sensitive to the insulin secretagogue properties of POA. Similar sensitivity was also observed in intracellular calcium mobilization experiments. Among many differences between human and mouse models of pancreatic β cells, negligible expression of *Gpr55* and *Gpr119* in MIN6 cells may be responsible for the need to use higher concentrations of POA isomers for insulin secretion.

One of the most important observations within this study was the different signal transduction pathway evoked by *c*POA and *t*POA. Surprisingly, we found that the *trans* isomer could effectively activate GPCR that couple through both Gq and Gs to increase intracellular Ca^{2+} and cAMP concentrations, respectively. However, in EndoC-βH1 cells treated with *t*POA and GPR119 antagonist we observed significant reduction of the cAMP level although under similar conditions insulin secretion was not decreased. Such discrepancy could result from other mechanisms not identified in this study. We discovered that GPR40 was most closely associated with the cAMP responses induced by *t*POA in EndoC-H1 cells. Such biased signaling, the existence of different ligand-dependent receptor coupling to diverse signaling effectors, has previously been observed for a small number of GPR40 agonists such as AM-1638 and AM-5262. Notably, two endogenous GPR40 ligands, α-linolenic acid and docosahexaenoic acid, were not able to significantly stimulate cAMP accumulation.[49] Therefore, our observations indicate for the first time that naturally occurring fatty acids can act as GPR40 biased agonists. Additionally, such biased signaling could be isomer-specific.

An *in silico* approach also indicated a slightly higher affinity of *t*POA for GPR40, GPR119, and GPR120 receptors. The *trans* stereoisomer is likely to create slightly more hydrophobic interactions with neighboring aromatic amino acid residues, which results in a subtle difference in binding affinity between selected ligands. Apparent discrepancy observed in the results of insulin secretion, Ca^{2+} mobilization and cAMP from the same experimental setup suggests that POA isomers can induce a differential receptor conformation, which activates a

different subset of signaling events, resulting in bias receptor signaling.

The different structures of the POA isomers can also change the membrane fluidity and spatial orientation of transmembrane proteins. This phenomenon can influence the activities of membrane proteins such as G-protein coupled receptors located in the plasma membrane.[27] Although *trans* fatty acids are unsaturated, their pi bonds are not kinked (degree of acyl chain bending) compared to *cis* pi bonds. Thus, when incorporated into membranes, they are expected to pack like saturated fatty acids, and a smaller pool of *trans* fatty acids will be incorporated into the membranes. Roach *et al.* reported that fatty acid chains with *trans* double bonds are straighter than "kinked" *cis* chains, thus affecting lipid packing.[67] Additionally, Cimen *et al.* postulated that *t*POA does not create the degree of acyl chain bending that the *cis* isomer does. Therefore, the effect of the double bond on physical membrane properties could be significantly diminished.[27] Their data showed that *t*POA can incorporate into the lipid pools more efficiently than *c*POA, leading to a 2–3 fold enrichment of this *trans*-fatty acid. However due to the *t*POA structure, its effects on membrane desaturation, organelle stress, and other effects are diminished compared to the impact caused by *c*POA. Therefore, it may be assumed that more tightly packed membranes containing *t*POA should be less permeable than the membranes with the *c*POA isomer, which are loosely packed and more permeable.[67]

5. Conclusions

Our studies show that *t*POA stimulates insulin secretion from mouse and human pancreatic β cells with a similar potency to that of *c*POA. Both palmitoleic acid isomers activate GPR40, GPR55, GPR119, and GPR120 receptors which mediate their augmentation of insulin secretion; however, not always statistically significant differences were demonstrated with the experiments with antagonists. Future studies should thoroughly characterize the role of GPCRs present in the pancreatic β cells in modulating the risk of diabetes by POA isomers. However, despite similar potency of activation, the intracellular signaling pathways are different. Taking into consideration the low cytotoxicity of *t*POA, this fatty acid could certainly have special and unique benefits to human health.

Our observations confirm the hypothesis that *trans*-palmitoleic acid may represent one of the bioactive components behind the insulin secretagogue properties of dairy products. Although *t*POA accounted for approx. 0.04% of total fatty acids in ruminant milk available at retail, the circulating plasma concentration of *t*POA reflects dairy fat consumption. Besides, although the percentage of *trans*-POA is very low in dairy food[9] and in the human body's circulation,[11] one can expect that foods fortified with *t*POA could be the way to increase its level in the human body, especially since recent studies showed that supplementation with sea buckthorn oil augmented in *t*POA increased serum phospholipid *t*POA.[12] This possibility is also supported by recent literature data reporting the synthesis of pure *t*POA on a larger scale. Guillocheau *et al.* demonstrated a method to obtain *t*POA from Provinal®, a dietary supplement with highly concentrated *c*POA. *c*POA was isolated by flash-LC and subjected to isomerization and *cis*/*trans* fractionation.[68] Alternatively, future studies can be undertaken on how to fortify milk fat with *t*POA by modifying a cow's diet as shown for *trans* fatty acids.[69]

Abbreviations

*c*POA	*cis*-Palmitoleic acid
FFA	Free fatty acids
GPCR	G protein-coupled receptor
GSIS	Glucose-stimulated insulin secretion
IBMX	3-Isobutyl-1-methylxanthine
POA	Palmitoleic acid
rTFA	Ruminant *trans* fatty acids
T2DM	Type 2 diabetes mellitus
*t*POA	*trans*-Palmitoleic acid

Author contributions

Eliza Korkus: investigation, methodology, and visualization; Marcin Szustak: investigation, methodology, and visualization; Rafal Madaj: investigation, methodology, and visualization; Arkadiusz Chworos: methodology and formal analysis; Anna Drzazga: investigation; Grzegorz Dąbrowski: investigation; Sylwester Czaplicki: investigation and methodology; Maria Koziołkiewicz: writing – original draft; Iwona Konopka: resources, conceptualization, and writing – original draft; Edyta Gendaszewska-Darmach: funding acquisition, conceptualization, formal analysis, writing – original draft, visualization, supervision, and project administration.

Conflicts of interest

There are no conflicts to declare.

Acknowledgements

This work was supported by a grant to EG-D. (2018/31/B/NZ9/02433) from The National Science Centre, Poland.

References

1 J. Guo, D. I. Givens, A. Astrup, S. J. L. Bakker, G. H. Goossens, M. Kratz, A. Marette, H. Pijl and S. S. Soedamah-Muthu, The Impact of Dairy Products in the Development of Type 2 Diabetes: Where Does the Evidence Stand in 2019?, *Adv. Nutr.*, 2019, **10**(6), 1066–1075, DOI: 10.1093/ADVANCES/NMZ050.

2 O. Hanus, E. Samkova, L. Křížova, L. Hasoňova and R. Kala, Role of Fatty Acids in Milk Fat and the Influence of Selected Factors on Their Variability—A Review, *Molecules*, 2018, **23**(7), 1636, DOI: **10.3390/molecules23071636**.

3 S. McGuire, U.S. Department of Agriculture and U.S. Department of Health and Human Services, Dietary Guidelines for Americans, 2010. 7th Edition, Washington, DC: U.S. Government Printing Office, January 2011, *Adv. Nutr.*, 2011, **2**(3), 293, DOI: **10.3945/AN.111.000430**.

4 L. Gijsbers, E. L. Ding, V. S. Malik, J. De Goede, J. M. Geleijnse and S. S. Soedamah-Muthu, Consumption of Dairy Foods and Diabetes Incidence: A Dose-Response Meta-Analysis of Observational Studies, *Am. J. Clin. Nutr.*, 2016, **103**(4), 1111–1124, DOI: **10.3945/AJCN.115.123216**.

5 E. Guillocheau, P. Legrand and V. Rioux, Trans-Palmitoleic Acid (Trans-9-C16:1, or Trans-C16:1 n-7): Nutritional Impacts, Metabolism, Origin, Compositional Data, Analytical Methods and Chemical Synthesis. A Review, *Biochimie*, 2020, **169**, 144–160, DOI: **10.1016/J.BIOCHI.2019.12.004**.

6 D. Mozaffarian, H. Cao, I. B. King, R. N. Lemaitre, X. Song, D. S. Siscovick and G. S. Hotamisligil, Circulating Palmitoleic Acid and Risk of Metabolic Abnormalities and New-Onset Diabetes, *Am. J. Clin. Nutr.*, 2010, **92**(6), 1350, DOI: **10.3945/AJCN.110.003970**.

7 E. Guillocheau, C. Garcia, G. Drouin, L. Richard, D. Catheline, P. Legrand and V. Rioux, Retroconversion of Dietary Trans-Vaccenic (Trans-C18:1 n-7) Acid to Trans-Palmitoleic Acid (Trans-C16:1 n-7): Proof of Concept and Quantification in Both Cultured Rat Hepatocytes and Pregnant Rats, *J. Nutr. Biochem.*, 2019, **63**, 19–26, DOI: **10.1016/J.JNUTBIO.2018.09.010**.

8 A. Haug, A. T. Høstmark and O. M. Harstad, Bovine Milk in Human Nutrition – a Review, *Lipids Health Dis.*, 2007, **6**(1), 1–16, DOI: **10.1186/1476-511X-6-25**.

9 F. Destaillats, R. L. Wolff, D. Precht and J. Molkentin, Study of Individual Trans- and Cis-16:1 Isomers in Cow, Goat, and Ewe Cheese Fats by Gas-Liquid Chromatography with Emphasis on the Trans-Δ3 Isomer, *Lipids*, 2000, **35**(9), 1027–1032, DOI: **10.1007/S11745-000-0614-Y**.

10 E. Guillocheau, C. Penhoat, G. Drouin, A. Godet, D. Catheline, P. Legrand and V. Rioux, Current Intakes of Trans-Palmitoleic (Trans-C16:1 n-7) and Trans-Vaccenic (Trans-C18:1 n-7) Acids in France Are Exclusively Ensured by Ruminant Milk and Ruminant Meat: A Market Basket Investigation, *Food Chem.: X*, 2020, **5**, 100081, DOI: **10.1016/J.FOCHX.2020.100081**.

11 D. Mozaffarian, H. Cao, I. B. King, R. N. Lemaitre, X. Song, D. S. Siscovick and G. S. Hotamisligil, Trans-Palmitoleic Acid, Metabolic Risk Factors, and New-Onset Diabetes in U.S. Adults: A Cohort Study, *Ann. Intern. Med.*, 2010, **153**(12), 790–799, DOI: **10.7326/0003-4819-153-12-201012210-00005**.

12 N. K. Huang, N. R. Matthan, J. M. Galluccio, P. Shi, A. H. Lichtenstein and D. Mozaffarian, Supplementation with Seabuckthorn Oil Augmented in 16:1n–7t Increases Serum Trans-Palmitoleic Acid in Metabolically Healthy Adults: A Randomized Crossover Dose-Escalation Study, *J. Nutr.*, 2020, **150**(6), 1388, DOI: **10.1093/JN/NXAA060**.

13 D. Mozaffarian, H. Cao and G. S. Hotamisligil, Use of Trans-Palmitoleate in Identifying and Treating Metabolic Disease, US8889739B2, 2011, **https://patents.google.com/patent/US8889739B2/en** (accessed 2022-06-08).

14 M. Y. Yakoob, P. Shi, W. C. Willett, K. M. Rexrode, H. Campos, E. J. Orav, F. B. Hu and D. Mozaffarian, Circulating Biomarkers of Dairy Fat and Risk of Incident Diabetes Mellitus Among Men and Women in the United States in Two Large Prospective Cohorts, *Circulation*, 2016, **133**(17), 1645–1654, DOI: **10.1161/CIRCULATIONAHA.115.018410**.

15 D. Mozaffarian, M. C. de Oliveira Otto, R. N. Lemaitre, A. M. Fretts, G. Hotamisligil, M. Y. Tsai, D. S. Siscovick and J. A. Nettleton, Trans-Palmitoleic Acid, Other Dairy Fat Biomarkers, and Incident Diabetes: The Multi-Ethnic Study of Atherosclerosis (MESA), *Am. J. Clin. Nutr.*, 2013, **97**(4), 854–861, DOI: **10.3945/AJCN.112.045468**.

16 I. D. Santaren, S. M. Watkins, A. D. Liese, L. E. Wagenknecht, M. J. Rewers, S. M. Haffner, C. Lorenzo and A. J. Hanley, Serum Pentadecanoic Acid (15:0), a Short-Term Marker of Dairy Food Intake, Is Inversely Associated with Incident Type 2 Diabetes and Its Underlying Disorders, *Am. J. Clin. Nutr.*, 2014, **100**(6), 1532–1540, DOI: **10.3945/AJCN.114.092544**.

17 J. Kröger, V. Zietemann, C. Enzenbach, C. Weikert, E. H. J. M. Jansen, F. Döring, H. G. Joost, H. Boeing and M. B. Schulze, Erythrocyte Membrane Phospholipid Fatty Acids, Desaturase Activity, and Dietary Fatty Acids in Relation to Risk of Type 2 Diabetes in the European Prospective Investigation into Cancer and Nutrition (EPIC)–Potsdam Study, *Am. J. Clin. Nutr.*, 2011, **93**(1), 127–142, DOI: **10.3945/AJCN.110.005447**.

18 L. I. Chávaro-Ortiz, B. D. Tapia, M. Rico-Hidalgo, R. Gutiérrez-Aguilar and M. E. Frigolet, Trans-Palmitoleic Acid Reduces Adiposity via Increased Lipolysis in a Rodent Model of Diet-Induced Obesity, *Br. J. Nutr.*, 2022, **127**(6), 801–809, DOI: **10.1017/S0007114521001501**.

19 D. T. Stein, B. E. Stevenson, M. W. Chester, M. Basit, M. B. Daniels, S. D. Turley and J. D. McGarry, The Insulinotropic Potency of Fatty Acids Is Influenced Profoundly by Their Chain Length and Degree of Saturation, *J. Clin. Invest.*, 1997, **100**(2), 398, DOI: **10.1172/JCI119546**.

20 J. Kraft, T. Jetton, B. Satish and D. Gupta, Dairy-Derived Bioactive Fatty Acids Improve Pancreatic ß-Cell Function, *FASEB J.*, 2015, **29**(S1), 608, DOI: **10.1096/FASEBJ.29.1_SUPPLEMENT.608.25**.

21 H. Cao, K. Gerhold, J. R. Mayers, M. M. Wiest, S. M. Watkins and G. S. Hotamisligil, Identification of a Lipokine, a Lipid Hormone Linking Adipose Tissue to Systemic Metabolism, *Cell*, 2008, **134**(6), 933, DOI: **10.1016/J.CELL.2008.07.048**.

22 L. Hodson, C. M. Skeaff and B. A. Fielding, Fatty Acid Composition of Adipose Tissue and Blood in Humans and

Its Use as a Biomarker of Dietary Intake, *Prog. Lipid Res.*, 2008, **47**(5), 348–380, DOI: **10.1016/J.PLIPRES.2008.03.003**.

23 L. Hodson and F. Karpe, Is There Something Special about Palmitoleate?, *Curr. Opin. Clin. Nutr. Metab. Care*, 2013, **16**(2), 225–231, DOI: **10.1097/MCO.0B013E32835D2EDF**.

24 G. Dąbrowski, S. Czaplicki, M. Szustak, E. Cichońska, E. Gendaszewska-Darmach and I. Konopka, Composition of Flesh Lipids and Oleosome Yield Optimization of Selected Sea Buckthorn (Hippophae Rhamnoides L.) Cultivars Grown in Poland, *Food Chem.*, 2022, **369**, 130921, DOI: **10.1016/J.FOODCHEM.2021.130921**.

25 E. Korkus, G. Dąbrowski, M. Szustak, S. Czaplicki, R. Madaj, A. Chworoś, M. Koziołkiewicz, I. Konopka and E. Gendaszewska-Darmach, Evaluation of the Anti-Diabetic Activity of Sea Buckthorn Pulp Oils Prepared with Different Extraction Methods in Human Islet EndoC-BetaH1 Cells, *NFS J.*, 2022, **27**, 54–66, DOI: **10.1016/J.NFS.2022.05.002**.

26 K. K. Alstrup, S. Gregersen, H. M. Jensen, J. L. Thomsen and K. Hermansen, Differential Effects of Cis and Trans Fatty Acids on Insulin Release from Isolated Mouse Islets, *Metabolism*, 1999, **48**(1), 22–29, DOI: **10.1016/S0026-0495(99)90005-7**.

27 I. Cimen, Z. Yildirim, A. E. Dogan, A. D. Yildirim, O. Tufanli, U. I. Onat, U. T. Nguyen, S. M. Watkins, C. Weber and E. Erbay, Double Bond Configuration of Palmitoleate Is Critical for Atheroprotection, *Mol. Metab.*, 2019, **28**, 58–72, DOI: **10.1016/J.MOLMET.2019.08.004**.

28 V. G. Tsonkova, F. W. Sand, X. A. Wolf, L. G. Grunnet, A. Kirstine Ringgaard, C. Ingvorsen, L. Winkel, M. Kalisz, K. Dalgaard, C. Bruun, J. J. Fels, C. Helgstrand, S. Hastrup, F. K. Öberg, E. Vernet, M. P. B. Sandrini, A. C. Shaw, C. Jessen, M. Grønborg, J. Hald, H. Willenbrock, D. Madsen, R. Wernersson, L. Hansson, J. N. Jensen, A. Plesner, T. Alanentalo, M. B. K. Petersen, A. Grapin-Botton, C. Honoré, J. Ahnfelt-Rønne, J. Hecksher-Sørensen, P. Ravassard, O. D. Madsen, C. Rescan and T. Frogne, The EndoC-BH1 Cell Line Is a Valid Model of Human Beta Cells and Applicable for Screenings to Identify Novel Drug Target Candidates, *Mol. Metab.*, 2018, **8**, 144–157, DOI: **10.1016/j.molmet.2017.12.007**.

29 E. Gendaszewska-Darmach, A. Drzazga and M. Koziołkiewicz, Targeting GPCRs Activated by Fatty Acid-Derived Lipids in Type 2 Diabetes, *Trends Mol. Med.*, 2019, **25**, 915–929, DOI: **10.1016/j.molmed.2019.07.003**.

30 K. F. McClure, E. Darout, C. R. W. Guimarães, M. P. Deninno, V. Mascitti, M. J. Munchhof, R. P. Robinson, J. Kohrt, A. R. Harris, D. E. Moore, B. Li, L. Samp, B. A. Lefker, K. Futatsugi, D. Kung, P. D. Bonin, P. Cornelius, R. Wang, E. Salter, S. Hornby, A. S. Kalgutkar and Y. Chen, Activation of the G-Protein-Coupled Receptor 119: A Conformation-Base Hypothesis for Understanding Agonist Response, *J. Med. Chem.*, 2011, **54**(6), 1948–1952, DOI: **10.1021/JM200003P/SUPPL_FILE/JM200003P_SI_001.PDF**.

31 J. Miyazaki, E. Yamato, T. Asano and K. Yamamura, Establishment of a Pancreatic Beta Cell Line That Retains Glucose-Inducible Insulin Secretion : Special Reference to Expression of Glucose Transporter, *Endocrinology*, 1990, **127**(1), 126–132, DOI: **10.1210/endo-127-1-126**.

32 P. Ravassard, Y. Hazhouz, S. Pechberty, E. Bricout-Neveu, M. Armanet, P. Czernichow and R. Scharfmann, A Genetically Engineered Human Pancreatic β Cell Line Exhibiting Glucose-Inducible Insulin Secretion, *J. Clin. Invest.*, 2011, **121**(9), 3589–3597, DOI: **10.1172/JCI58447**.

33 P. Bergsten and B. Hellman, Glucose-Induced Amplitude Regulation of Pulsatile Insulin Secretion from Individual Pancreatic Islets, *Diabetes*, 1993, **42**(5), 670–674, DOI: **10.2337/diab.42.5.670**.

34 S. Jo, T. Kim, V. G. Iyer and W. Im, CHARMM-GUI: A Web-Based Graphical User Interface for CHARMM, *J. Comput. Chem.*, 2008, **29**(11), 1859–1865, DOI: **10.1002/JCC.20945**.

35 A. T. McNutt, P. Francoeur, R. Aggarwal, T. Masuda, R. Meli, M. Ragoza, J. Sunseri and D. R. Koes, GNINA 1.0: Molecular Docking with Deep Learning, *J. Cheminf.*, 2021, **13**(1), 1–20, DOI: **10.1186/S13321-021-00522-2/FIGURES/13**.

36 D. A. Case, K. Belfon, I. Y. Ben-Shalom, S. R. Brozell, D. S. Cerutti, T. E. Cheatham I, V. W. D. Cruzeiro, T. A. Darden, R. E. Duke, G. Giambasu, M. K. Gilson, H. Gohlke, A. W. Goetz, R. Harris, S. Izadi, S. A. Izmailov, K. Kasavajhala, A. Kovalenko, R. Krasny, T. Kurtzman, T. S. Lee, S. LeGrand, P. Li, C. Lin, J. Liu, T. Luchko, R. Luo, V. Man, K. M. Merz, Y. Miao, O. Mikhailovskii, G. Monard, H. Nguyen, A. Onufriev, F. Pan, S. Pantano, R. Qi, D. R. Roe, A. Roitberg, C. Sagui, S. Schott-Verdugo, J. Shen, C. L. Simmerling, N. R. Skrynnikov, J. Smith, J. Swails, R. C. Walker, J. Wang, L. Wilson, R. M. Wolf, X. Wu, Y. Xiong, Y. Xue, D. M. York and P. A. Kollman, *AMBER 2020*, University of California, San Francisco, 2020.

37 C. Tian, K. Kasavajhala, K. A. A. Belfon, L. Raguette, H. Huang, A. N. Migues, J. Bickel, Y. Wang, J. Pincay, Q. Wu and C. Simmerling, Ff19SB: Amino-Acid-Specific Protein Backbone Parameters Trained against Quantum Mechanics Energy Surfaces in Solution, *J. Chem. Theory Comput.*, 2020, **16**(1), 528–552, DOI: **10.1021/ACS.JCTC.9B00591/SUPPL_FILE/CT9B00591_SI_002.ZIP**.

38 K. K. Grotz and N. Schwierz, Magnesium Force Fields for OPC Water with Accurate Solvation, Ion-Binding, and Water-Exchange Properties: Successful Transfer from SPC/E, *J. Chem. Phys.*, 2022, **156**(11), 114501, DOI: **10.1063/5.0087292**.

39 C. J. Dickson, R. C. Walker and I. R. Gould, Lipid21: Complex Lipid Membrane Simulations with AMBER, *J. Chem. Theory Comput.*, 2022, **18**(3), 1726–1736, DOI: **10.1021/ACS.JCTC.1C01217/SUPPL_FILE/CT1C01217_SI_001.PDF**.

40 D. Vassetti, M. Pagliai and P. Procacci, Assessment of GAFF2 and OPLS-AA General Force Fields in Combination with the Water Models TIP3P, SPCE, and OPC3 for the Solvation Free Energy of Druglike Organic Molecules, *J. Chem. Theory Comput.*, 2019, **15**(3), 1983–1995, DOI: **10.1021/ACS.JCTC.8B01039/ASSET/IMAGES/LARGE/CT-2018-01039Z_0008.JPEG**.

41 R. J. Woods and R. Chappelle, Restrained Electrostatic Potential Atomic Partial Charges for Condensed-Phase Simulations of Carbohydrates, *J. Mol. Struct.: THEOCHEM*,

2000, **527**(1–3), 149–156, DOI: **10.1016/S0166-1280(00)00487-5**.

42 J. Wang, W. Wang, P. A. Kollman and D. A. Case, Automatic Atom Type and Bond Type Perception in Molecular Mechanical Calculations, *J. Mol. Graphics Modell.*, 2006, **25**(2), 247–260, DOI: **10.1016/J.JMGM.2005.12.005**.

43 J. Zou, C. Tian and C. Simmerling, Blinded Prediction of Protein–Ligand Binding Affinity Using Amber Thermodynamic Integration for the 2018 D3R Grand Challenge 4, *J. Comput. Aided Mol. Des.*, 2019, **33**(12), 1021–1029, DOI: **10.1007/S10822-019-00223-X/FIGURES/5**.

44 S. Lenz, I. Bodnariuc, M. Renaud-Young, T. M. Shandro and J. L. MacCallum, *FABP7 Binds to Fatty Acid Micelles: Implications for Lipid Transport*, 2021. DOI: **10.1101/2021.10.22.465361**.

45 D. R. Perinelli, M. Cespi, N. Lorusso, G. F. Palmieri, G. Bonacucina and P. Blasi, Surfactant Self-Assembling and Critical Micelle Concentration: One Approach Fits All?, *Langmuir*, 2020, **36**(21), 5745–5753, DOI: **10.1021/ACS.LANGMUIR.0C00420/ASSET/IMAGES/LARGE/LA0C00420_0006.JPEG**.

46 M. A. Partearroyo, H. Ostolaza, F. M. Goñi and E. Barberá-Guillem, Surfactant-Induced Cell Toxicity and Cell Lysis. A Study Using B16 Melanoma Cells, *Biochem. Pharmacol.*, 1990, **40**(6), 1323–1328, DOI: **10.1016/0006-2952(90)90399-6**.

47 A. Drzazga, E. Cichońska, M. Koziołkiewicz and E. Gendaszewska-Darmach, Formation of BTC3 and MIN6 Pseudoislets Changes the Expression Pattern of Gpr40, Gpr55, and Gpr119 Receptors and Improves Lysophosphatidylcholines-Potentiated Glucose-Stimulated Insulin Secretion, *Cells*, 2020, **9**(9), 2062, DOI: **10.3390/cells9092062**.

48 A. Hirasawa, K. Tsumaya, T. Awaji, S. Katsuma, T. Adachi, M. Yamada, Y. Sugimoto, S. Miyazaki and G. Tsujimoto, Free Fatty Acids Regulate Gut Incretin Glucagon-like Peptide-1 Secretion through GPR120, *Nat. Med.*, 2005, **11**(1), 90–94, DOI: **10.1038/NM1168**.

49 M. Hauge, M. A. Vestmar, A. S. Husted, J. P. Ekberg, M. J. Wright, J. Di Salvo, A. B. Weinglass, M. S. Engelstoft, A. N. Madsen, M. Lückmann, M. W. Miller, M. E. Trujillo, T. M. Frimurer, B. Holst, A. D. Howard and T. W. Schwartz, GPR40 (FFAR1) – Combined Gs and Gq Signaling in Vitro Is Associated with Robust Incretin Secretagogue Action Ex Vivo and in Vivo, *Mol. Metab.*, 2015, **4**(1), 3, DOI: **10.1016/J.MOLMET.2014.10.002**.

50 C. M. Henstridge, N. A. Balenga, R. Schröder, J. K. Kargl, W. Platzer, L. Martini, S. Arthur, J. Penman, J. L. Whistler, E. Kostenis, M. Waldhoer and A. J. Irving, GPR55 Ligands Promote Receptor Coupling to Multiple Signalling Pathways, *Br. J. Pharmacol.*, 2010, **160**(3), 604, DOI: **10.1111/J.1476-5381.2009.00625.X**.

51 A. C. Kaushik, A. Kumar, A. U. Rehman, M. Junaid, A. Khan, S. Bharadwaj, S. Sahi and D.-Q. Wei, *Deciphering G-Protein-Coupled Receptor 119 Agonists as Promising Strategy against Type 2 Diabetes Using Systems Biology Approach*, 2018. DOI: **10.1021/acsomega.8b01941**.

52 G. Carullo, S. Mazzotta, M. Vega-Holm, F. Iglesias-Guerra, J. M. Vega-Pérez, F. Aiello and A. Brizzi, GPR120/FFAR4 Pharmacology: Focus on Agonists in Type 2 Diabetes Mellitus Drug Discovery, *J. Med. Chem.*, 2021, **64**, 4332, DOI: **10.1021/acs.jmedchem.0c01002**.

53 A. Srivastava, J. Yano, Y. Hirozane, G. Kefala, F. Gruswitz, G. Snell, W. Lane, A. Ivetac, K. Aertgeerts, J. Nguyen, A. Jennings and K. Okada, High-Resolution Structure of the Human GPR40 Receptor Bound to Allosteric Agonist TAK-875, *Nature*, 2014, **513**(7516), 124–127, DOI: **10.1038/nature13494**.

54 G. Gocheva, N. Ivanova, S. Iliev, J. Petrova, G. Madjarova and A. Ivanova, Characteristics of a Folate Receptor-α Anchored into a Multilipid Bilayer Obtained from Atomistic Molecular Dynamics Simulations, *J. Chem. Theory Comput.*, 2020, **16**(1), 749–764, DOI: **10.1021/ACS.JCTC.9B00872/SUPPL_FILE/CT9B00872_SI_002.ZIP**.

55 C. S. Sum, I. G. Tikhonova, S. Neumann, S. Engel, B. M. Raaka, S. Costanzi and M. C. Gershengorn, Identification of Residues Important for Agonist Recognition and Activation in GPR40, *J. Biol. Chem.*, 2007, **282**(40), 29248–29255, DOI: **10.1074/JBC.M705077200**.

56 J. Lu, N. Byrne, J. Wang, G. Bricogne, F. K. Brown, H. R. Chobanian, S. L. Colletti, J. Di Salvo, B. Thomas-Fowlkes, Y. Guo, D. L. Hall, J. Hadix, N. B. Hastings, J. D. Hermes, T. Ho, A. D. Howard, H. Josien, M. Kornienko, K. J. Lumb, M. W. Miller, S. B. Patel, B. Pio, C. W. Plummer, B. S. Sherborne, P. Sheth, S. Souza, S. Tummala, C. Vonrhein, M. Webb, S. J. Allen, J. M. Johnston, A. B. Weinglass, S. Sharma and S. M. Soisson, Structural Basis for the Cooperative Allosteric Activation of the Free Fatty Acid Receptor GPR40, *Nat. Struct. Mol. Biol.*, 2017, **24**(7), 570–577, DOI: **10.1038/nsmb.3417**.

57 O. Elbegdorj, R. B. Westkaemper and Y. Zhang, A Homology Modeling Study toward the Understanding of Three- Dimensional Structure and Putative Pharmacological Profile of the G-Protein Coupled Receptor GPR55, *J. Mol. Graphics Modell.*, 2013, **39**, 50–60, DOI: **10.1002/aur.1474.Replication**.

58 M. A. Lingerfelt, P. Zhao, H. P. Sharir, D. P. Hurst, P. H. Reggio and A. Me, Identification of Crucial Amino Acid Residues Involved in Agonist Signaling at the GPR55 Receptor, *Biochemistry*, 2016, **56**(3), 473–486, DOI: **10.1021/acs.biochem.6b01013**.

59 A. Drzazga, A. Sowińska, A. Krzemińska, A. Okruszek, P. Paneth, M. Koziołkiewicz and E. Gendaszewska-Darmach, 2-OMe-Lysophosphatidylcholine Analogues Are GPR119 Ligands and Activate Insulin Secretion from BTC-3 Pancreatic Cells: Evaluation of Structure-Dependent Biological Activity, *Biochim. Biophys. Acta, Mol. Cell Biol. Lipids*, 2018, **1863**(1), 91–103, DOI: **10.1016/J.BBALIP.2017.10.004**.

60 M. S. Engelstoft, C. Norn, M. Hauge, N. D. Holliday, L. Elster, J. Lehmann, R. M. Jones, T. M. Frimurer and T. W. Schwartz, Structural Basis for Constitutive Activity

and Agonist-Induced Activation of the Enteroendocrine Fat Sensor GPR119, *Br. J. Pharmacol.*, 2014, **171**(24), 5774–5789, DOI: **10.1111/bph.12877**.

61 M. Takeuchi, A. Hirasawa, T. Hara, I. Kimura, T. Hirano, T. Suzuki, N. Miyata, T. Awaji, M. Ishiguro and G. Tsujimoto, FFA1-Selective Agonistic Activity Based on Docking Simulation Using FFA1 and GPR120 Homology Models, *Br. J. Pharmacol.*, 2013, **168**(7), 1570–1583, DOI: **10.1111/j.1476-5381.2012.02052.x**.

62 B. D. Hudson, B. Shimpukade, G. Milligan and T. Ulven, The Molecular Basis of Ligand Interaction at Free Fatty Acid Receptor 4 (FFA4/GPR120), *J. Biol. Chem.*, 2014, **289**(29), 20345–20358, DOI: **10.1074/JBC.M114.561449**.

63 T. Nagasawa, M. Horitani, S. i. Kawaguchi, S. Higashiyama, Y. Hama and S. Mitsutake, The Molecular Mechanism of Phytosphingosine Binding to FFAR4/GPR120 Differs from That of Other Fatty Acids, *FEBS Open Bio*, 2021, **11**(11), 3081–3089, DOI: **10.1002/2211-5463.13301**.

64 R. Usui, D. Yabe, M. Fauzi, H. Goto, A. Botagarova, S. Tokumoto, H. Tatsuoka, Y. Tahara, S. Kobayashi, T. Manabe, Y. Baba, T. Kurosaki, P. L. Herrera, M. Ogura, K. Nagashima and N. Inagaki, GPR40 Activation Initiates Store-Operated Ca2+ Entry and Potentiates Insulin Secretion via the IP3R1/STIM1/Orai1 Pathway in Pancreatic β-Cells, *Sci. Rep.*, 2019, **9**(1), 1–11, DOI: **10.1038/s41598-019-52048-1**.

65 K. Kurotani, M. Sato, Y. Ejima, A. Nanri, S. Yi, N. M. Pham, S. Akter, K. Poudel-Tandukar, Y. Kimura, K. Imaizumi and T. Mizoue, High Levels of Stearic Acid, Palmitoleic Acid, and Dihomo-γ-Linolenic Acid and Low Levels of Linoleic Acid in Serum Cholesterol Ester Are Associated with High Insulin Resistance, *Nutr. Res.*, 2012, **32**(9), 669–675, DOI: **10.1016/J.NUTRES.2012.07.004**.

66 X. Tong, C. Dai, J. T. Walker, G. G. Nair, A. Kennedy, R. M. Carr, M. Hebrok, A. C. Powers and R. Stein, Lipid Droplet Accumulation in Human Pancreatic Islets Is Dependent on Both Donor Age and Health, *Diabetes*, 2020, **69**(3), 342–354, DOI: **10.2337/DB19-0281/-/DC1**.

67 C. Roach, S. E. Feller, J. A. Ward, S. R. Shaikh, M. Zerouga and W. Stillwell, Comparison of Cis and Trans Fatty Acid Containing Phosphatidylcholines on Membrane Properties, *Biochemistry*, 2004, **43**(20), 6344–6351, DOI: **10.1021/BI049917R**.

68 E. Guillocheau, G. Drouin, D. Catheline, C. Orione, P. Legrand and V. Rioux, Chemical Synthesis and Isolation of Trans-Palmitoleic Acid (Trans-C16:1 n-7) Suitable for Nutritional Studies, *Eur. J. Lipid Sci. Technol.*, 2020, **122**(6), 1900409, DOI: **10.1002/EJLT.201900409**.

69 J. M. Chardigny, C. Malpuech-Brugère, F. Dionisi, D. E. Bauman, B. German, R. P. Mensink, N. Combe, P. Chaumont, D. M. Barbano, F. Enjalbert, J. B. Bezelgues, I. Cristiani, J. Moulin, Y. Boirie, P. A. Golay, F. Giuffrida, J. L. Sébédio and F. Destaillats, Rationale and Design of the TRANSFACT Project Phase I: A Study to Assess the Effect of the Two Different Dietary Sources of Trans Fatty Acids on Cardiovascular Risk Factors in Humans, *Contemp. Clin. Trials*, 2006, **27**(4), 364–373, DOI: **10.1016/J.CCT.2006.03.003**.